


ORIGINAL ARTICLE

CFD analysis on optimizing the annular fin parameters toward an improved storage response in a triple-tube containment system

Abdullah Bahlekeh¹ | Hayder I. Mohammed² | Waleed Khalid Al-Azzawi³ | Anmar Dulaimi⁴ | Hasan Sh. Majdi⁵ | Pouyan Talebizadehsardari⁶ | Jasim M. Mahdi⁷ 

¹Mechanical Engineering Department, Ege University, Bornova/Izmir, Turkey

²Department of Physics, College of Education, University of Garmian, Kalar, Iraq

³Department of Medical Instrumentation Engineering Techniques, Al-Farahidi University, Baghdad, Iraq

⁴College of Engineering, University of Warith Al-Anbiyaa, Karbala, Iraq

⁵Department of Chemical Engineering and Petroleum Industries, Al-Mustaqbal University College, Babylon, Iraq

⁶Centre for Sustainable Energy Use in Food Chains, Institute of Energy Futures, Brunel University London, London, UK

⁷Department of Energy Engineering, University of Baghdad, Baghdad, Iraq

Correspondence

Jasim M. Mahdi, Department of Energy Engineering, University of Baghdad, Baghdad 10071, Iraq.
 Email: jasim.m@uob.edu.iq

Abstract

Due to the low thermal conductivity of the phase change material and low thermal diffusion inside the phase change material, this study seeks to improve the melting response of a triple-tube latent heat storage system via employing annular fins by optimizing their structural parameters, including the fin number, location, and dimensions. Natural convection effects are numerically evaluated considering different numbers and the locations of the fins, including fin numbers of 4, 10, 16, 20, and 30 in a vertical system orientation. The fins are attached to the inner and outer sides of the annulus, accommodating the phase change material between the inner and center tubes. The fins' number and location are identical on both sides of the annulus, and the volume of the fins is the same across all scenarios evaluated. The results show that the higher the number of fins used, the greater the heat communication between the fins and the phase change material layers in charge, resulting in faster melting and a higher rate of heat storage. Due to the limited natural convection effect and lower heat diffusion at the heat exchanger's bottom, an additional fin is added, and its thickness is assessed. The results show that the case with equal fin thickness, that is, both original fins and the new fin, performs the best performance compared with that for the cases with an added fin with thicknesses of 0.5, 1, and 2 mm. Eliminating an extra fin from the base of the system for the case with 30 fins increases the charging time by 53.3%, and reduces the heat storage rate by 44%. The overall melting time for the case with an added fin to the bottom is 1549 s for the case with 30 fins which is 85.8%, 34.2%, 18%, and 8.8% faster than the cases with 4, 10, 16, and 20 fins, respectively. This study reveals that further attention should be given to the position and number of annular fins to optimize the melting mechanism in phase-changing materials-based heat storage systems.

KEYWORDS

melting, natural convection, number and arrangement of fins, phase change material, thermal energy storage, triple-tube latent heat storage system

1 | INTRODUCTION

Renewable energy sources have received much attention due to the limited sources of fossil fuels and their environmental pollution consequences.¹ The performance of renewable energy systems such as solar collectors can be improved by incorporating thermal energy storage (TES) components.² There are three schemes for conserving thermal energy, the sensible, the latent, and the thermochemical TES.³ The latent heat energy storage scheme (LHESS) is superior to the other forms of storing thermal energy due to these reasons⁴: (a) thermal energy is held at a constant temperature,⁵ (b) the energy storage density of LHESS is higher than that of the others,⁶ and (c) LHESS can operate in a large number of cycles without any significant limitation.⁷ LHESS is mostly recommended in applications with space limitations since thermal energy can be stored 5–14 times greater than that of sensible heat storage materials.^{8,9} Because the heat conductivity of nearly all phase-changing materials (PCMs) is generally low, resulting in a lower heat conduction rate, more extended energy storage, and retrieval durations in the LHESS.^{10,11} Various research has been accomplished to improve heat conduction transfer in the LHESS. Conduction heat transfer can be improved via multiple enhancement techniques, including the utilization of fins,^{12–21} metal foams,^{22–26} nanoparticles,^{27–30} nanoencapsulating PCMs,^{31–33} multiple PCMs,^{34–37} and heat pipes.^{38,39} It should be mentioned that special considerations should be taken since applying enhancement techniques in the LHESS may change the flow regime, increasing weight and reducing the required space for the PCM. Although the PCM-based heat storage could be employed in plane enclosures with no fin,^{40,41} adding fins can improve the thermal response of PCMs more efficiently as compared to other techniques such as applying nanoparticles,⁴² metal wool,⁴³ and high-temperature packed bed system.^{44,45}

A series of experimental and computational studies were carried out to evaluate the fins' impact characteristics such as the number of fins' length, orientation angle, and thickness on the thermal response in TES systems.⁴⁶ Hosseini et al.⁴⁷ conducted an experimental and numerical study to investigate the impact of longitudinal fins on the thermal characteristics of a PCM storage system. The results showed that fins extension resulted in deeper penetration of heat into the PCM and consequently, the melting time was reduced. Wang et al.⁴⁸ accomplished a numerical study to investigate the melting process of PCM in a sleeve-tube system in the

presence of internal fins. The influences of fins geometry including, the angle between fins, fin length, and fin ratio as well as conductivity of outer tube on the PCM melting phenomenon, were analyzed. They deduced that outer tube conductivity played a significant role in the melting process. Furthermore, the melting process was highly improved by increasing the fin's length rather than the fin's thickness. Kamkari and Groulx⁷ ran several experiments to evaluate the effects of adding fins in rectangular enclosures under various inclination angles. The experimental results showed that the melting phenomenon was highly dependent on the inclination angle rather than on adding fins. It should be mentioned that reducing the inclination angle accelerated the melting phenomenon. Yazici et al.⁴⁹ achieved an experimental analysis to evaluate the impacts of inclination angle as well as fin number on the thermal characteristics of a PCM-based heat sink. The experimental results showed that variation of the inclination angle from 0° to 60° increased the operating time by 83.4%. They finally concluded that the thermal performance of the case with three fins and an inclination angle of 60° was the best. Kalbasi et al.⁵⁰ accomplished a numerical analysis to determine the optimum PCM volume fraction as well as the optimum fins number in a finned PCM-based heat sink. They evaluated the regression model rationality using the variance analysis. It was deduced that increasing the fin's thickness decreased the optimal fin number. Furthermore, an increase in heat flux value increased the optimal fins number. Yan et al.^{51,52} numerically investigated the heat transfer efficiency in a fractal microchannel and they found that increasing the initial velocity and nanoparticles' loading leads to an improved heat transfer at the expense of pressure loss. Yao and Huang⁵³ introduced a novel triangular fin to enhance the discharging process of a triplex-tube TES unit. They discussed the impacts of triangular fin positions on the solidification performance of the unit in detail. The study outcomes reveal that the optimal triangular fin could reduce the solidification time of the TES unit by 30.98%. Sodhi and Muthukumar⁵⁴ developed a numerical study to enhance heat transfer of a vertical-oriented shell and tube LHESS via using nonuniform fin distribution. The TES system was comprised of three types of PCMs with various melting points of 360°C, 335.8°C, and 305.4°C. They reported that discharging and charging time of the multiple-PCM system was equal to or less than that of the system with a single PCM for Ste_{ref} (Stefan number) ≥ 1 . Wang et al.⁵⁵ studied the feasibility of using L-shaped fin to boost the charging process

of a vertical-oriented PCM-based enclosure. Two scenarios were considered in their research: (1) positioning the fins at the lower side of the enclosure and (2) positioning the fins at the upper side of the enclosure. They deduced that energy storage capacity, melting performance, and exergy of the enclosure were highly influenced by the dimensions and orientation of the L-shaped fins. Desai et al.⁵⁶ conducted a numerical study to evaluate the efficacy of inverted fin configurations in reducing the peak temperature of a PCM-based thermal control system. They investigated the effects of various parameters including cross-section, mass, shape, and number of fins on the thermal characteristics of the PCM-based system. They concluded that the peak temperature was the lowest for the case with the novel inverted fins. Luo et al.⁵⁶ accomplished a numerical study to evaluate the potential of using combined fractal fins in enhancing the thermal performance of a PCM-based heat exchanger. The effects of various parameters including the fins spacing, bifurcation level, heat transfer area, and mixed types of

fractal fins on the charging process of the PCM-based unit were investigated. The findings showed that the total melting time of the case with combined fractal fins was reduced by 68% in comparison with that of the case with the conventional fractal fins. Mao et al.^{57,58} studied the effect of the tank structure and the fin configuration on the thermal efficiency of the TES. They indicated that as the number of fins increases, the total heat storage time is shorter, but the total heat storage has also been reduced. Furthermore, the review of prior literature revealed that, despite extensive research on the functionality of the finned-tube heat exchanger as a functional PCM confinement design, there are no studies that adequately examine dependant parameters such as the number, location, and dimensions of the fins. No extra material is used in such a design, so there is no additional cost. Consequently,

TABLE 1 The proposed cases including the number and the dimensions of the fins.

Case	Fin number	Dimension of the fins
Case 1	4	5 mm × 5 mm
Case 2	10	2 mm × 5 mm
Case 3	16	1.25 mm × 5 mm
Case 4	20	1 mm × 5 mm
Case 5	30	0.65 mm × 5 mm

TABLE 4 Thermodynamic properties of the PCM used.³⁰

Properties	Values
ρ_l (kg/m ³)	770
ρ_s (kg/m ³)	860
C_p (kJ/kg K)	170
L_f (kJ/kg)	2
K (W/m K)	0.2
μ (N s/m ²)	0.023
T_L (°C)	36
T_S (°C)	29
β (J/K)	0.0006

TABLE 2 The dimension of the fins in different thicknesses for case-5 fins and adding a flat fin to the bottom of the PCM container.

Case	Added fins thickness (mm)	Number of fins	Dimension of fins (mm ²)	Dimension of the added fin (mm ²)
Case 2-AF-1	0.5	11	1.8 × 5	0.5 × 20
Case 2-AF-2	1	11	1.6 × 5	1 × 20
Case 2-AF-3	2	11	1.2 × 5	2 × 20
Case 2-AF-4	Same thickness	11	1.43 × 5	1.43 × 20

TABLE 3 The proposed cases with added fins including the number and the dimensions of the fins.

Case	Fin number	Dimension (mm ²)	Added-fin dimension (mm ²)
Case 1-AF	5	2.5 × 5	2.5 × 20
Case 2-AF	11	1.43 × 5	1.43 × 20
Case 3-AF	17	1 × 5	1 × 20
Case 4-AF	21	0.82 × 5	0.82 × 20
Case 5-AF	31	0.58 × 5	0.58 × 20

this design could be considered a more efficient economical configuration. Thus, studying and evaluating the best location and number of fins gives further information and knowledge in this field. This study's major goal was to numerically assess the efficiency of a finned triple-tube LHTES to boost the melting rate and enhance the thermal rate released from the HTF. The number and the spacing between the fins were optimized to gain a higher charging rate. Natural convection affects the entire charging mechanism, expressed tacitly in the article, considering the simultaneous effect of the fin's addition.

Moreover, the effects of an added fin to the bottom of the heat exchanger using various thicknesses are also evaluated to improve the natural convection effect. The evaluation is achieved by exploring the liquid phase development, the melting rate, the contours of the phases, and the temperature. This study aims to attain the fin's position through the PCM domain to reach the best location and take the maximum benefit of free convective flows to raise the melting rate.

2 | MODELING, MESH STUDY, AND VALIDATION

2.1 | Mathematical modeling

To simulate the phase change phenomenon in the PCM domain, the enthalpy–porosity approach is selected to be used in this study. The conservation equations stipulated by the phase transition limitations, which include the mass, momentum, and energy, are summarized as follows depending on the enthalpy–porosity approach developed by Brent et al.⁵⁹:

$$\frac{\partial \rho}{\partial t} + \nabla \times \rho \vec{V} = 0, \quad (1)$$

$$\rho \frac{\partial \vec{V}}{\partial t} + \rho (\vec{V} \times \nabla) \vec{V} = -\nabla P + \mu (\nabla^2 \vec{V}) - \rho_{\text{ref}} \beta (T - T_{\text{ref}}) \vec{g} - \vec{S}, \quad (2)$$

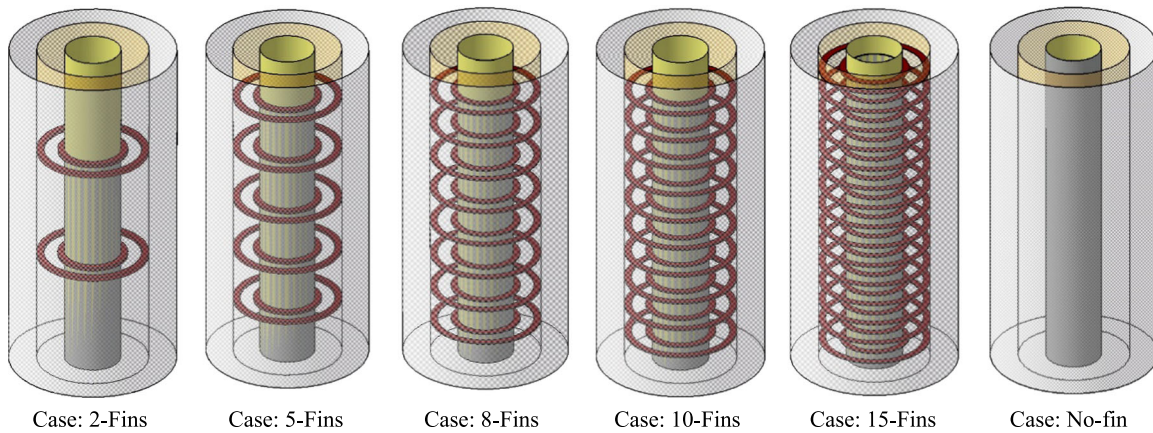


FIGURE 1 The schematic of the proposed systems with different numbers of the fins.

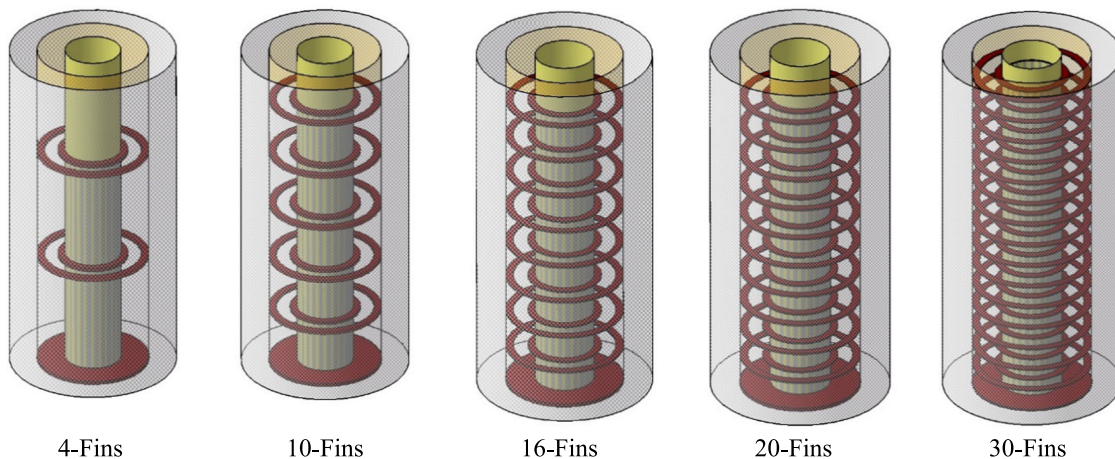


FIGURE 2 The schematic of the proposed systems with a different number of fins and an added fin to the bottom of the heat exchanger.

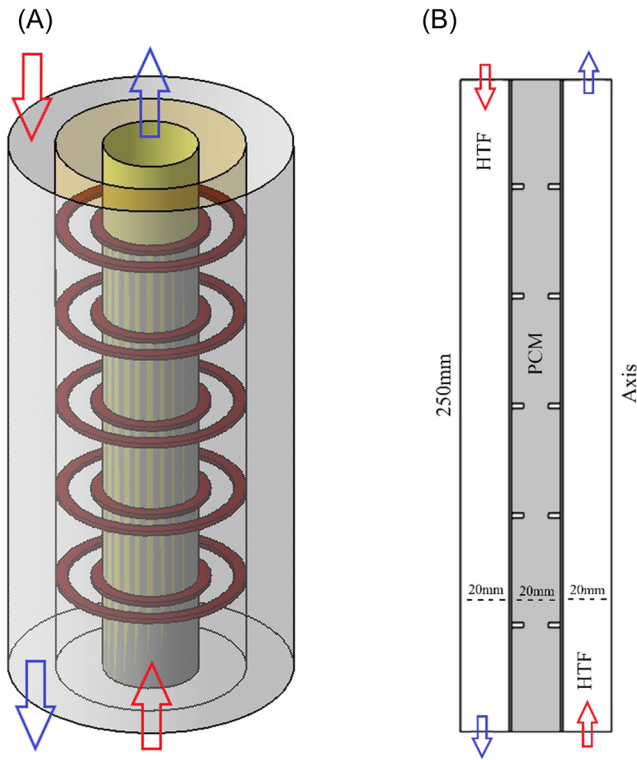


FIGURE 3 The boundary conditions and dimensions of the proposed system in (A) full domain and (B) axisymmetric condition.

where Boussinesq approximation $[\rho = \rho_{\text{ref}}\beta(T - T_{\text{ref}})]$ is applied by taking into account the natural convection effect in the momentum equation with V is the fluid velocity, P is the pressure, T is the temperature, and S is a source term²⁵:

$$\vec{S} = A_m \frac{(1 - \lambda)^2}{\lambda^3 + 0.001} \vec{V}, \quad (3)$$

where $A_m = 10^5$ as the mushy zone parameter and λ is the PCM liquid fraction.^{60–63} The energy equation is derived as²⁵:

$$\frac{\rho C_p \partial T}{\partial t} + \nabla(\rho C_p \vec{V} T) = \nabla(k \nabla T) - S_L. \quad (4)$$

The source term S_L is obtained as⁶⁴:

$$S_L = \frac{\partial \rho \lambda L_f}{\partial t} + \nabla(\rho \vec{V} \lambda L_f), \quad (5)$$

where λ is introduced as²⁰:

$$\lambda = \frac{\Delta H}{L_f} = \begin{cases} 0 & \text{if } T < T_{\text{Solidus}} \\ 1 & \text{if } T > T_{\text{Liquidus}} \\ \frac{T - T_{\text{Solidus}}}{T_{\text{Liquidus}} - T_{\text{Solidus}}} & \text{if } T_{\text{Solidus}} < T < T_{\text{Liquidus}} \end{cases}, \quad (6)$$

where ΔH is the latent heat component for PCM that may vary between zero for solid PCM and L_f (the latent heat of melting) for liquid PCM.

It is worth noting that the governing equations are developed based on the following assumptions⁶⁵:

1. Newtonian, transient and incompressible fluid for the liquid PCM.
2. No volume change for the PCM during melting.

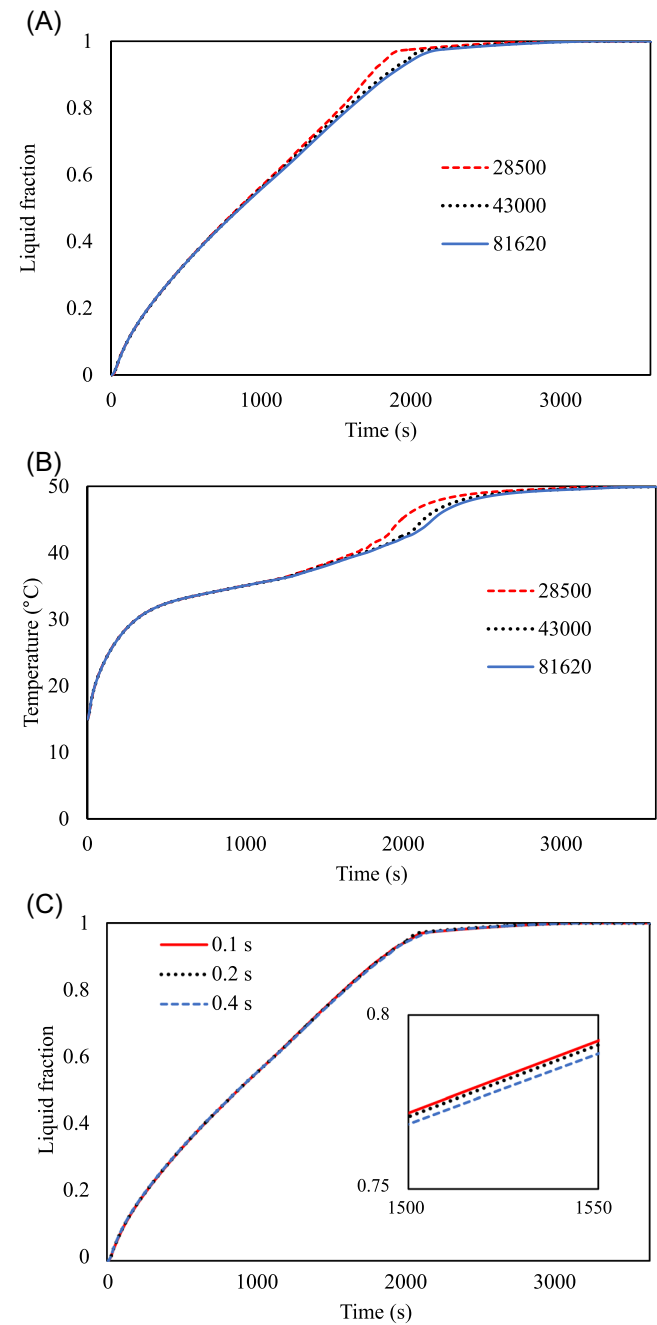


FIGURE 4 (A) liquid fraction and (B) mean temperature of PCM for different grid sizes, and (C) liquid fraction profile for various time step sizes.

3. The density variation is accounted for by the Boussinesq technique.
4. The PCM has constant characteristics except for density.
5. Consider Ignorable viscous dissipation.

The rate of heat storage or recovery \dot{Q} is also defined as⁶⁶:

$$\dot{Q} = \frac{Q}{t_m} = \frac{m \left(\int_{\text{solid}} c_p dT + L_f + \int_{\text{liquid}} c_p dT \right)}{t_m} \quad (7)$$

$$\approx \frac{m(c_p(T_L - T_i) + L_f + c_p(T_e - T_s))}{t_m},$$

where Q is the heat capacity during the storage or recovery mode and t_m is the melting or solidification time upon the phase completion.

3 | PROBLEM DESCRIPTION

This study aims to study the number of fins in a vertical triple-pipe latent heat storage (LHS) system. The fins are placed in the PCM domain which is situated at the center tube while the HTF domain is inner and outer pipes. The

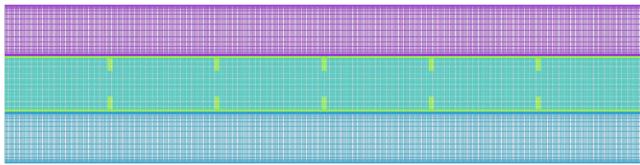


FIGURE 5 The mesh arrangement after the grid independence analysis (using 43,000 cells).

length of the heat storage unit is 250 mm while the inner and outer tube diameters are 20 and 40 mm, respectively, which are chosen based on different studies in the literature.¹⁶ Thus, the system can be described as follows for the PCM and HTF domains:

3.1 | PCM domain

Different fins' numbers of 4, 10, 16, 20, and 30 are proposed to enhance heat transfer in the PCM domain and from the HTF to the PCM. The fins are connected to the pipe's interior and exterior sides inside the PCM domain. The number and location of the fins are similar for the inside and center tubes. Figure 1 displays the schematic of the studied systems compared with the plain fin triple pipe system.

Table 1 lists the dimensions of the fins for different studied systems. In all the proposed cases, the mass of the PCM and the volume of the fins are considered constant. Thus, the thickness of the fins is calculated to achieve these conditions. The height of the fins is considered constant, equal to 5 mm.

In the previous paper of the authors,²⁸ it was shown that due to the natural convection effect in a vertical heat storage system during the phase change process, the PCM at the upper section of the storage system is melted faster than the PCM at the bottom. Thus, adding a rectangular fin to the bottom of the heat exchanger was recommended to increase the heat transfer rate. In the study by Ghalambaz et al.,²⁸ the thickness of the added fin to the bottom of the heat exchanger is considered constant equal to 1 mm; however, in this study, for the case with 10 fins, different thicknesses of 0.5, 1, 2, and the case of the same thickness with the other fins are examined to study the effect of added fin thickness. In all cases, the thickness of other fins is calculated to have

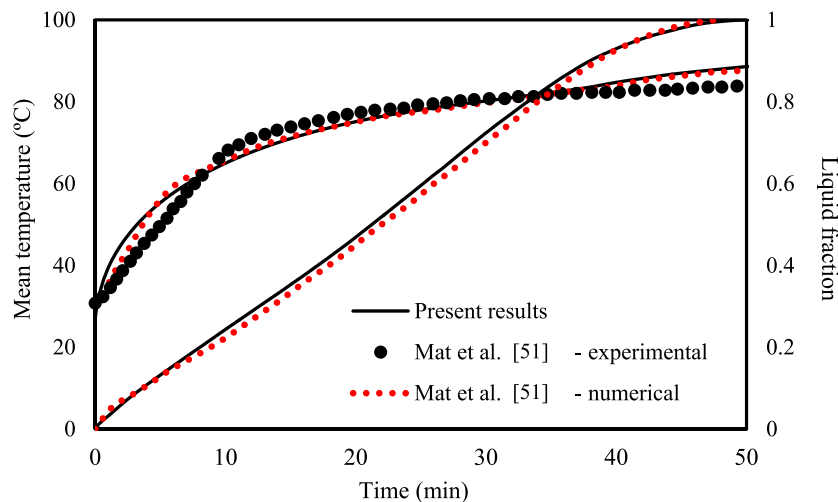


FIGURE 6 Code verification compared with the data of Mat et al.⁶⁰

equal PCM mass and fin volume. Table 2 presents the dimensions of the fins for different cases. In Table 2, the same thickness means that the thicknesses of all fins (the added fin and the rest 10 fins) are equal, as shown in Table 3.

After analyzing the thickness of the added fin, which is discussed later, the case of the same thickness has the best performance with a negligible difference from the case with

the fin thickness of 1 mm. Thus, the effect of fins' numbers is studied for the proposed cases. The proposed systems' schematics are displayed in Figure 2, and the dimensions of the fins are listed in Table 3. It should be noted that the added fin's size is considered equal to the dimensions of the other fins, and thus the thickness of the fins in the case with the added fin is different from that of the case without added

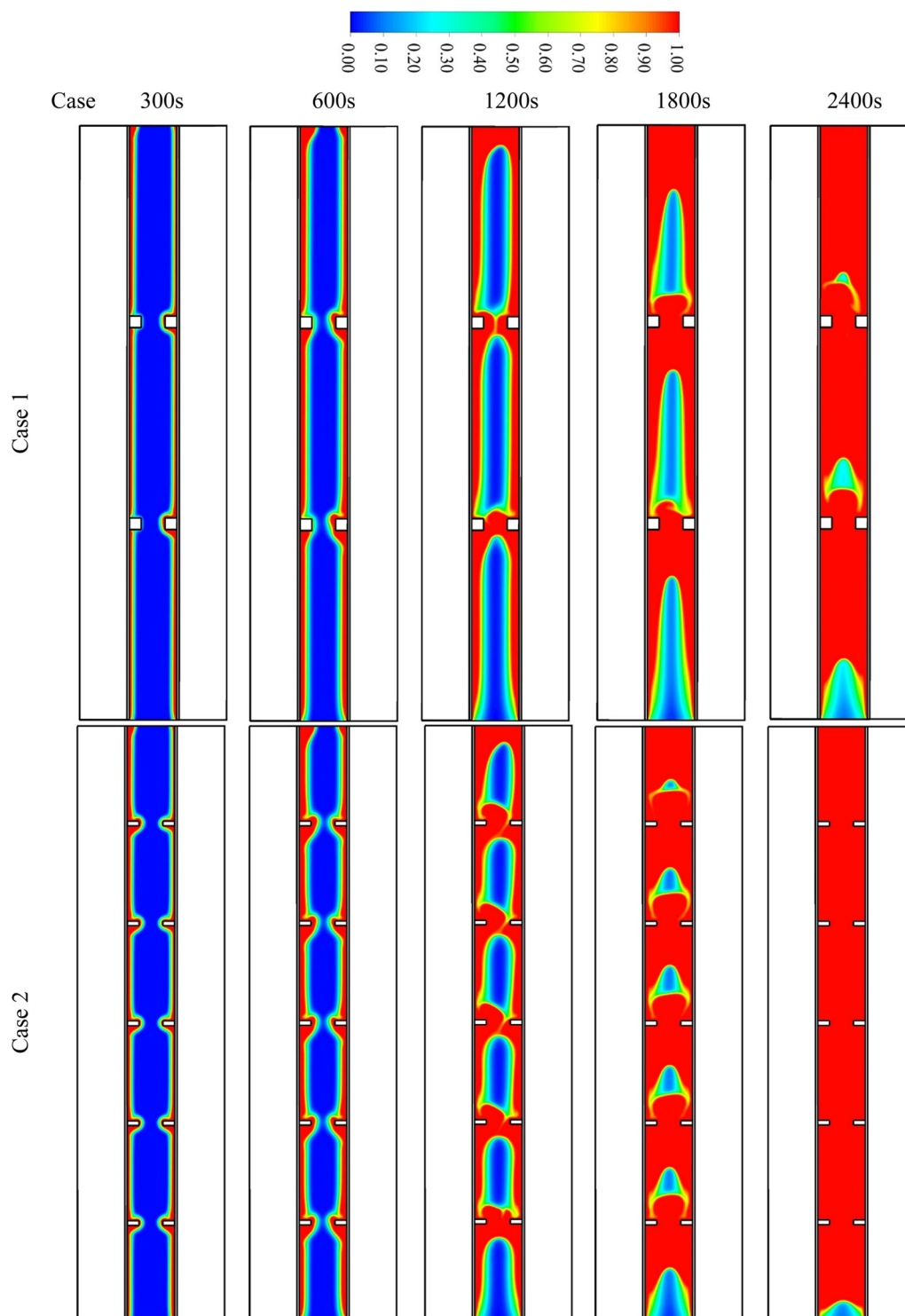


FIGURE 7 The liquid fraction development in Cases 1–5 at different time steps.

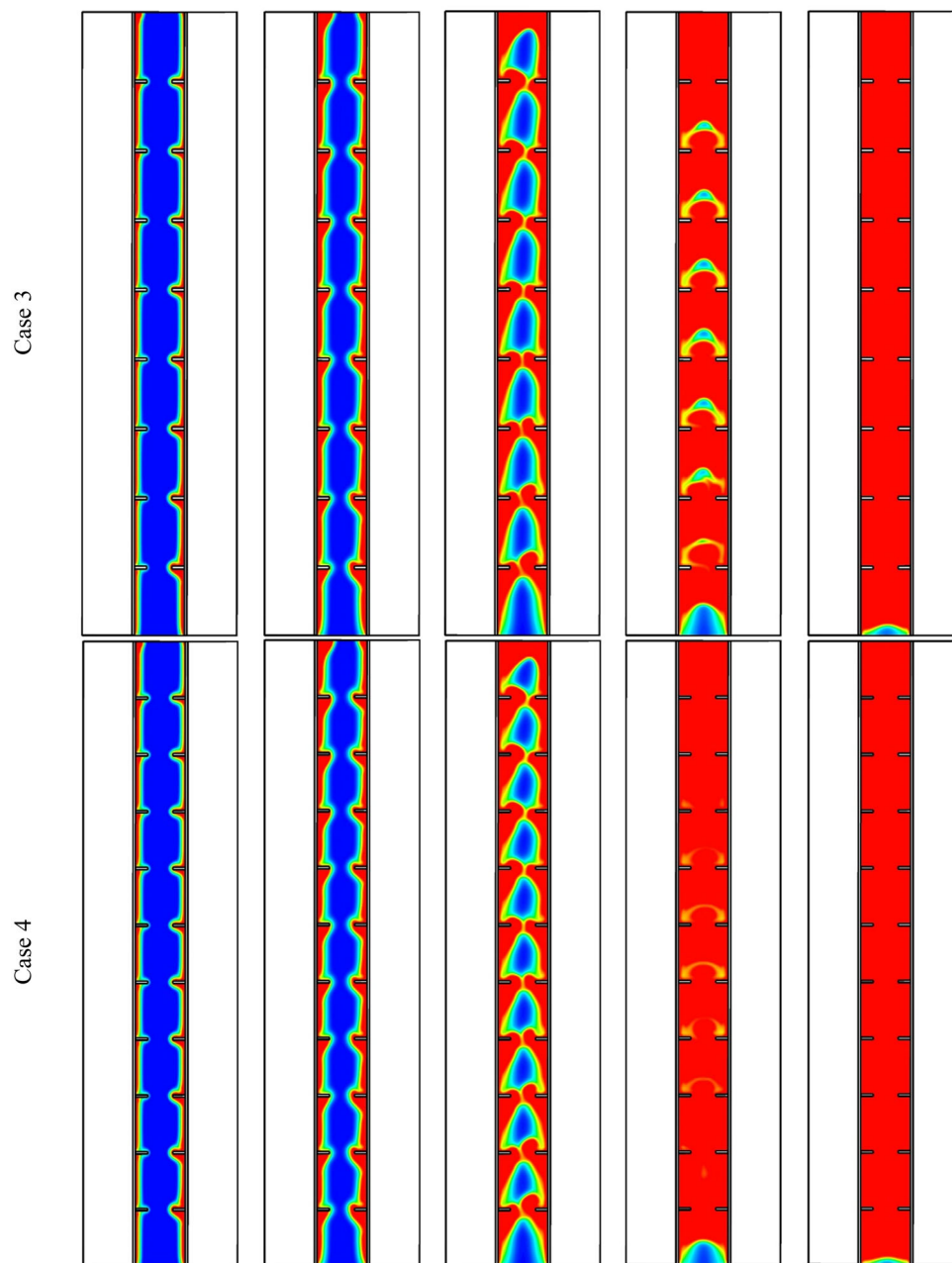


FIGURE 7 Continued

fin. Also, note that Case 2-AF in Table 3 is the same as Case 2-AF-4 in Table 2.

Paraffin RT-35 is used in the present study. The melting temperature of this PCM is suitable for HVAC applications. The properties of RT-35 are presented in Table 4.

3.2 | HTF domain

As recommended in the literature, when melting is the mode in the triple pipe heat exchanger, the HTF should be circulated in the opposite direction of gravity in the

inner pipe while it is in the gravity direction of the outer tube. This means that the flow of the HTF in the heat exchanger should be countercurrent during the melting process.²⁹ The dimensions of the system and the flow directions are displayed in Figure 3 for the finned case with 10 fins. The pipes' inner, middle, and outer hydraulic diameters are 40 mm, and the height of the heat exchanger is 250 mm. Because of the nature and characteristics of the system under consideration, as well as the absence of circumferential flow variation, the fluid flow and heat transfer are evaluated in an axisymmetric condition for this study.

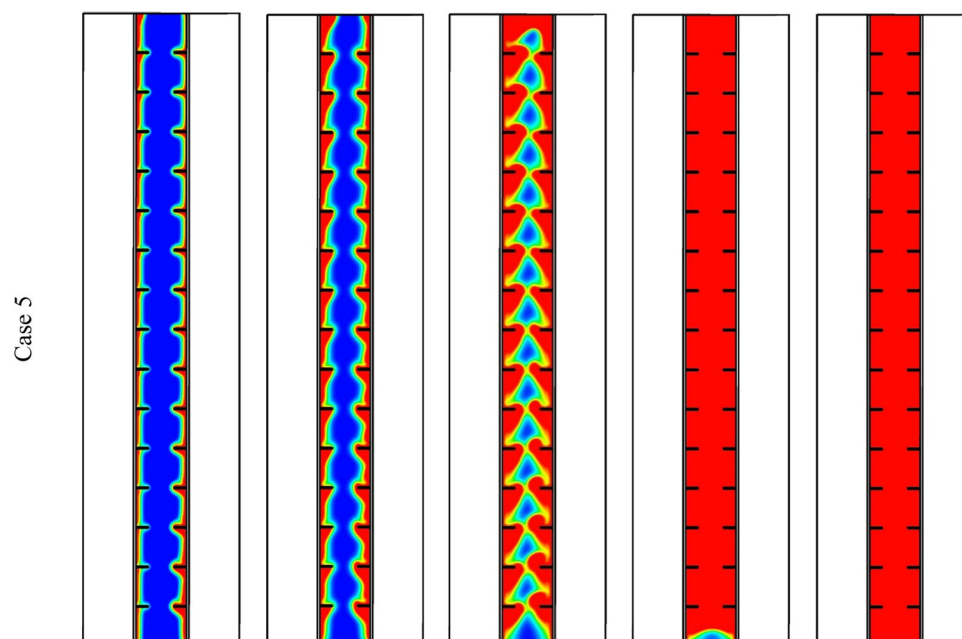


FIGURE 7 Continued

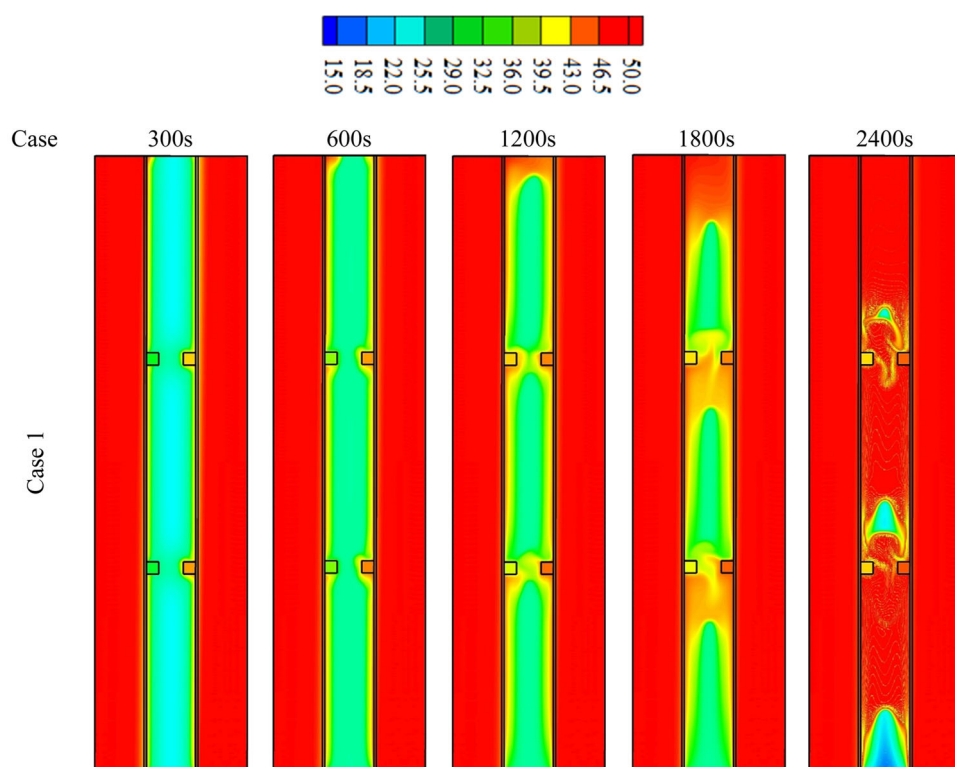


FIGURE 8 The temperature contours in Cases 1–5 at different times.

4 | NUMERICAL MODEL, MESH STUDY, AND VALIDATION

ANSYS workbench 18.1 is adopted to conduct the CFD simulation, mesh construction, and numerical analysis. Also, the QUICK scheme is adopted to estimate

diffusion and convection fluxes, while the PRESTO scheme is utilized to solve the pressure correction equation. Convergence conditions are also set out as 10^{-6} for iterations on all governing equations. In addition, mesh independence was investigated, and the independence of time step size. For the finned cases

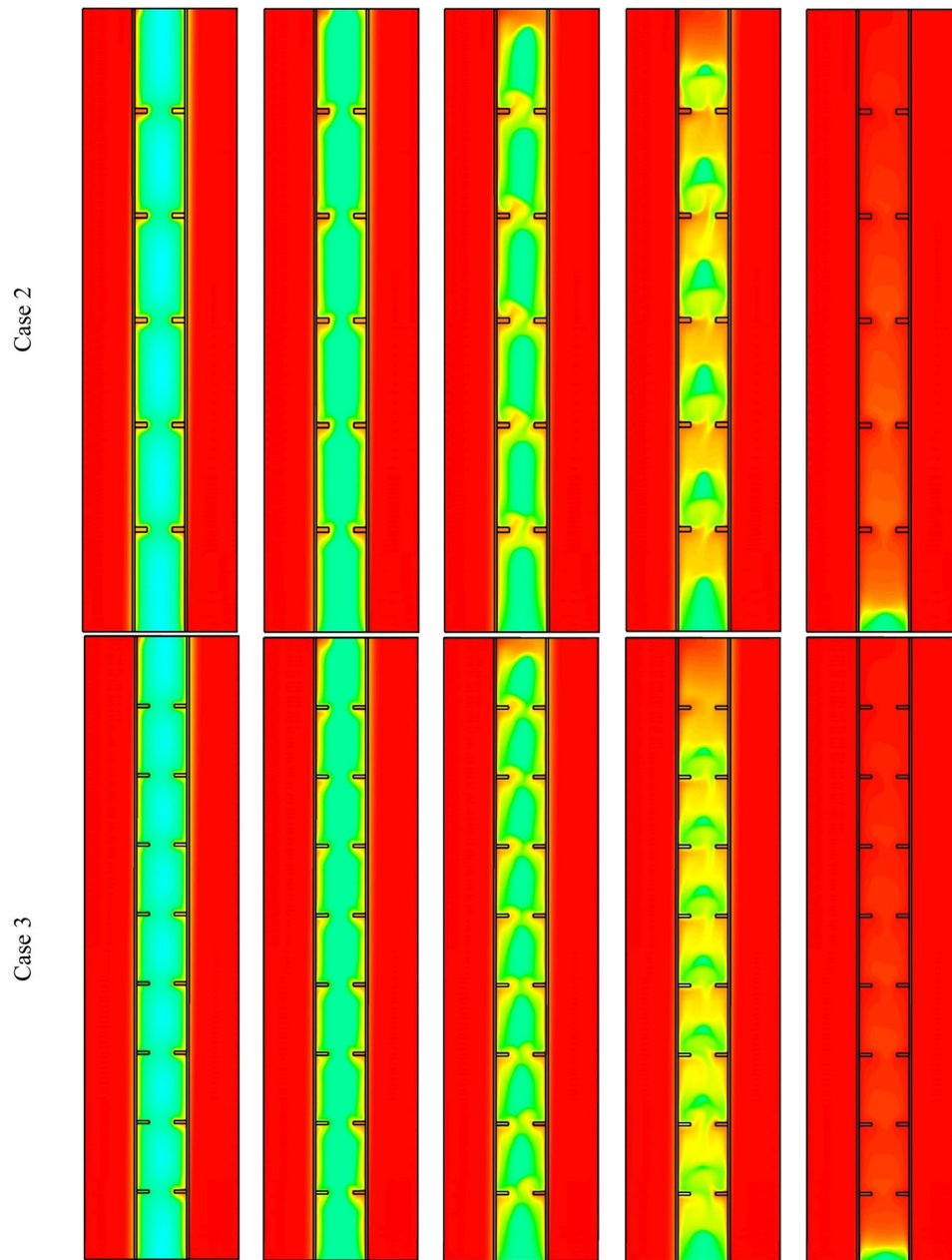


FIGURE 8 Continued

with uniform fin arrangement, a time step size of 0.2 s is used to examine the mesh independency of various mesh sizes. The number of cells varies from 28,500 to 81,620 depending on the mesh size. Figure 4A,B illustrate the variation in liquid fraction and mean temperature for different meshing cell sizes. Because the results are almost similar for cell sizes 43,000 and 81,620, mesh size 43,000 is chosen for the remaining analyses. Figure 1C illustrates the volatility of the liquid fraction for different time step sizes for the specified grid size. As can be observed, the results are almost identical for the time step sizes of 0.1, 0.2, and 0.4 s, particularly for 0.2 and 0.1 s values.

Consequently, the time step size has been set at 0.2 s in this investigation. It should be noted that for evaluating the grid size and time step size, the Reynolds number of 1000 and the inlet water temperature of 50°C were used to represent the HTF boundary conditions at the intake section.

Figure 5 shows the mesh adopted after the mesh independence test, which has 43,000 cells.

The developed CFD code was validated using the experimental findings of Mat et al.⁶⁰ on temperature and liquid fraction, as well as their numerical predictions. In their study, Mat et al.⁶⁰ evaluated a finned double-tube LHSHE unit with TR58 acting as the PCM with water as

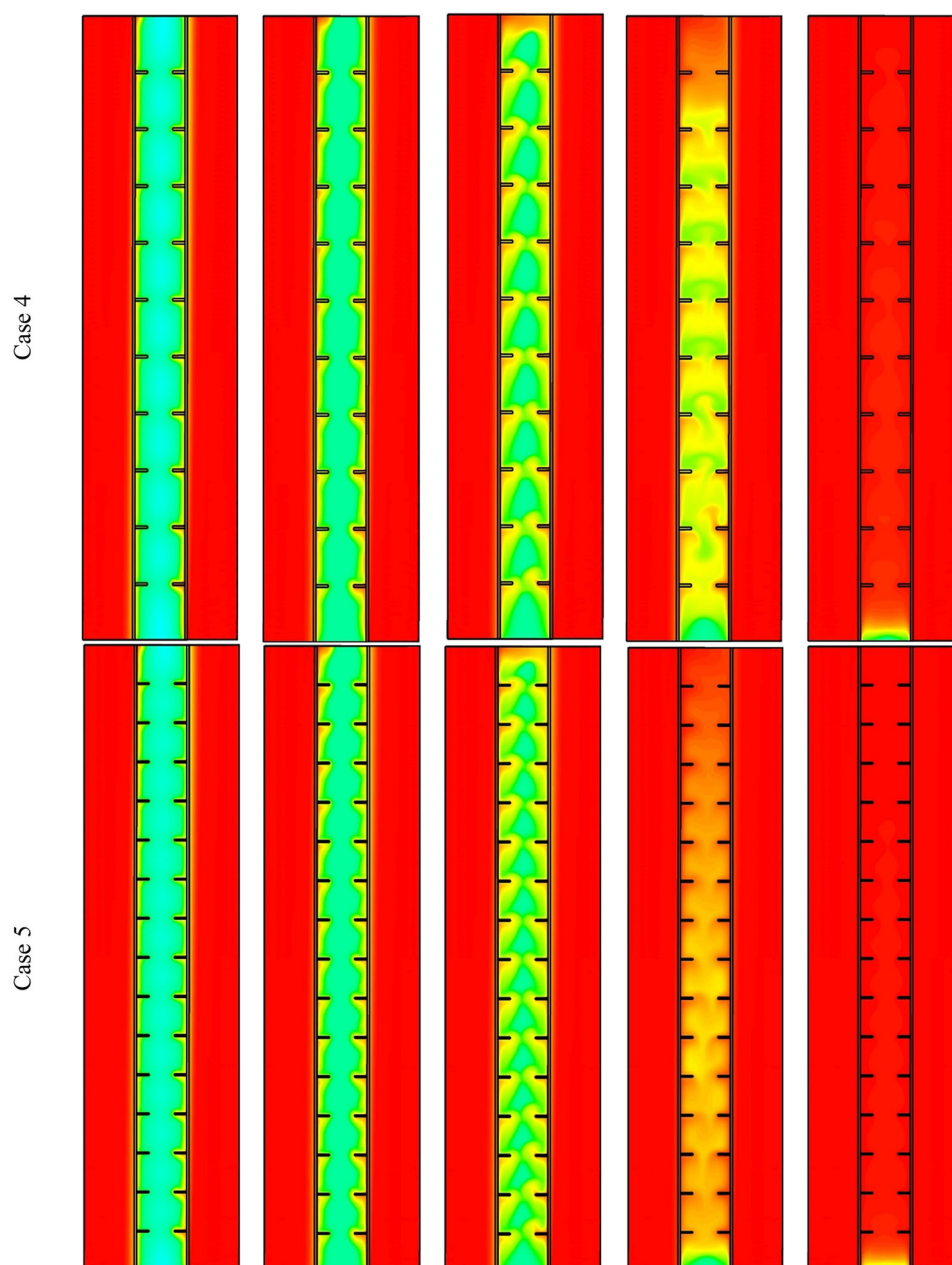


FIGURE 8 Continued

the HTF for achieving the required boundary conditions of constant wall temperature on the PCM domain. The same boundary conditions and performance parameters of the reference system are applied in the present model. The objective of their research was to evaluate the impacts of adding staggered fins to the exterior and interior walls of the PCM shell. As can be observed in Figure 6, there is a significant deal of consistency when the present results are compared to those of Mat et al.⁶⁰ The statistical validation gave a maximum percentage error of 1.4%. It should be noted that the experimental uncertainty in the study of Mat et al.⁶⁰ is $\pm 0.15^\circ\text{C}$ (around 0.2%) for the temperature measurement.

5 | RESULTS AND DISCUSSION

This section investigates the impacts of different numbers and dimensions of the fins on the melting procedure of a PCM-based heat storage system. To obtain the optimized pattern, four different cases are studied for the five fins case considering adding a fin to the bottom of the unit and utilizing various fins' thicknesses of 0.5, 1, 2, and the same thickness (unifying the thickness of the fins and the added fin to the bottom). In the last section, the effects of fins' numbers in the case with an added fin to the bottom are studied to find the optimum configuration. It is

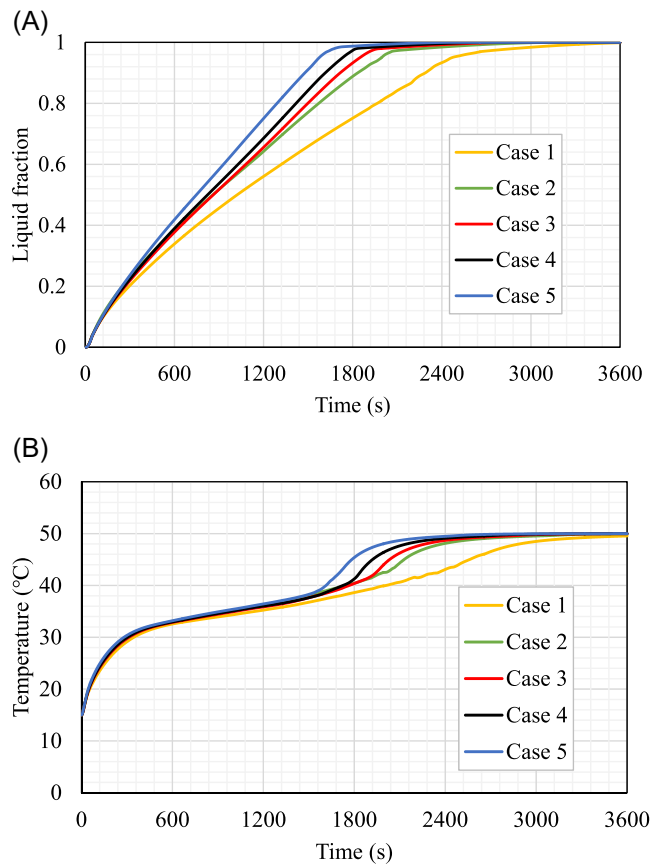


FIGURE 9 (A) Liquid fraction, (B) average temperature profiles for Cases 1, 2, 3, 4, and 5 during the melting process.

TABLE 5 The total melting time and the heat storage rate for different cases of the fins number during the melting process.

	Melting time (s)	Heat storage rate (W)
Case 1	3661	45.96
Case 2	3056	55.05
Case 3	2796	60.16
Case 4	2626	64.04
Case 5	2375	70.76

worthwhile noting that the total volume for all the fins is the same to guarantee the utilization of the same volume of the PCM in the system and also to make a reasonable comparison according to the fins' addition. Note that to name different cases, only the number of fins on one wall of the heat exchanger is counted.

This study presents a new contribution in this field as a step ahead to establishing an efficient finned triple-tube heat storage unit by applying an optimal fin array in the system. The primary key of this study is to reveal the competence of using many fins instead of applying few to

the system. The results are analyzed by comparing the liquid fractions, temperature distributions, melting rates, and heat storage rates of various cases.

5.1 | Effect of the number of fins

Combining fins with the LHESS improves the thermal unit's efficiency by expanding the thermal exchange surface area. Boosting the mean thermal conductivity of the unit by applying a high thermally conductive metal fin likewise performs the leading role in enhancing efficiency. The fins act as a thermal delivery from the inner and outer sides to the deep parts of PCM. Besides, the fins significantly impact the natural convection heat transfer as they create an obstacle against the molten PCM circulation. Five different numbers of pairs of fins are integrated into the shell side of the unit on both inner and outer parts. All the considered cases are stated in Table 1. The cross-section areas of the fins for all the cases are the same (100 mm^2), to guarantee utilization of the same PCM volume, and all the fins are in a horizontal direction (inline). The first case is equipped with two square fins on each side (four fins on both sides) with dimensions of $5 \text{ mm} \times 5 \text{ mm}$ (Case 1), and the second case includes five rectangular fins (10 fins on both sides) with dimensions of $2 \text{ mm} \times 5 \text{ mm}$ (Case 2). The length of the fins for the first five cases is constant (5 mm), while the thickness and the number of the fins are varied. The third, fourth, and fifth cases include 8, 10, and 15 fine on each side (16, 20, and 30 fins on both sides, respectively) with dimensions of $1.25 \text{ mm} \times 5 \text{ mm}$, $1 \text{ mm} \times 5 \text{ mm}$, and $0.65 \text{ mm} \times 5 \text{ mm}$, respectively, presenting Cases 3, 4, and 5.

Figure 7 illustrates the liquid fraction contours for the cases above at various times of 300, 600, 1200, 1800, and 2400 s. For all the cases, the PCM initially melts at the attached area of the wall and around the fins. During the first 300 s, the adjacent PCM to the inner and outer HTF channel walls is melted due to the conduction heat transfer, which is the primary heat transfer mechanism since most PCM is solid. The molten area expands gradually with time due to gaining more heat from the walls and the fins. The cases practically present the same behavior, and the solid part is confined between the two neighbor fins. The molten PCM expands more within 600 s, and the solid parts between the fins are about to separate in the region between the opposite fins' inline pair. Over time, other PCM melts, forming a thicker liquid layer, which covers the solid part and gathers at the top because of the natural convection. At 1200 s, all the solid parts are separated in the region between the opposite inline fins. The molten PCM expands more and cover the most area

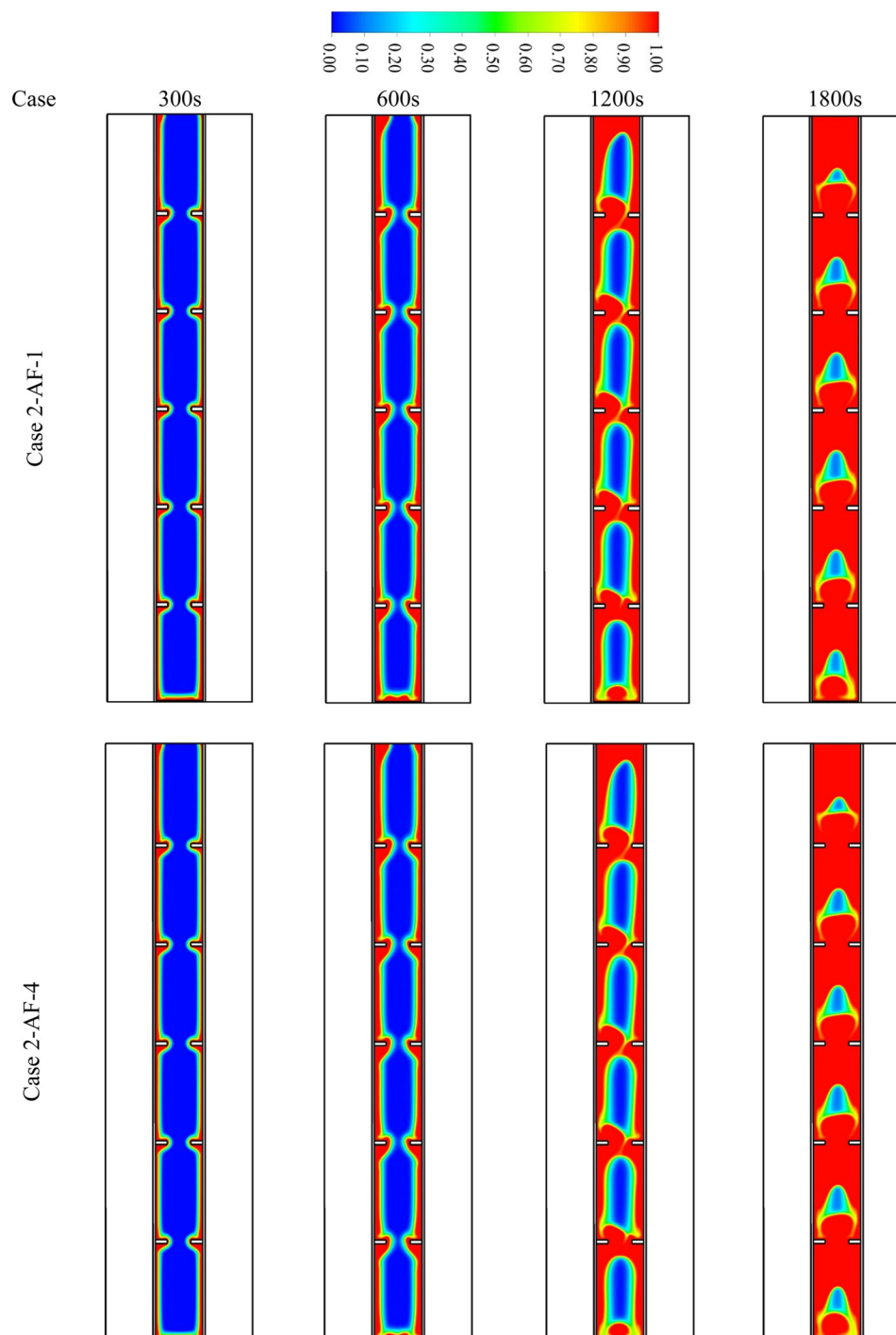


FIGURE 10 The liquid fraction development contours in Case 2-AF-1, Case 2-AF-2, Case 2-AF-3, and Case 2-AF-4.

for all the cases (with different ratio) at 1800 s. The solid fraction's value reduces with increasing the number of fins, whereas the liquid fraction reaches 0.75 for Case 1, and 0.98 for Case 5, and the only portion of the solid-state remains at the bottom of the heat exchanger. The entire PCM melts within 2400 s in Case 5, however, just 93% is melted during this time for Case 1 while 99% is melted for Case 4 at the same time duration. This

conduct returns to the larger surface area which provides by increasing the number of the fins, whereas the surface area increases by five times considering Case 1 compared with Case 5. The distribution of the fins also has a great impact on the phase change process, since the heat transfer occurs more homogeneously on the one hand, and on the other hand, with increasing the number of the fins, the lowest fin becomes closer to the

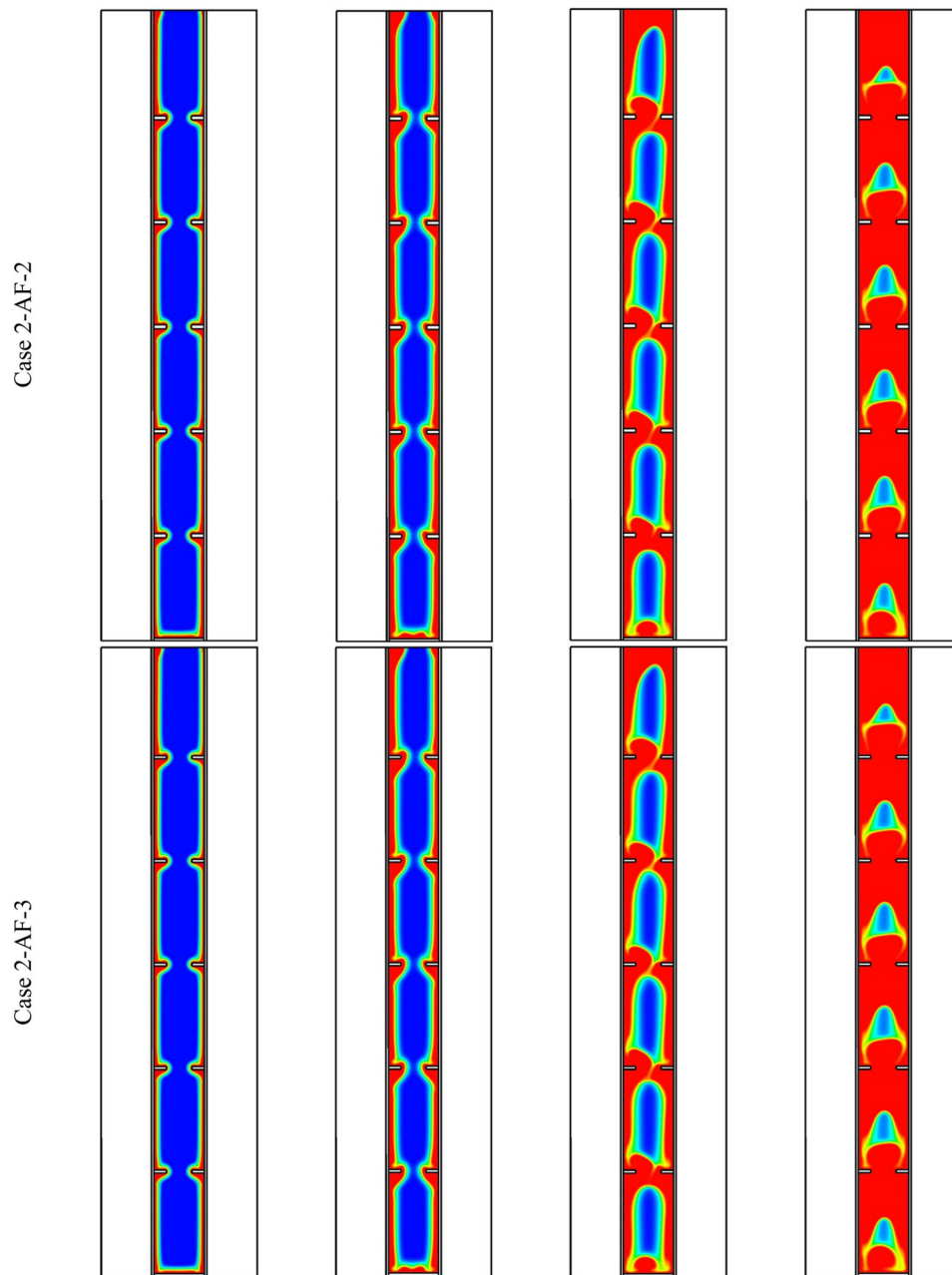


FIGURE 10 Continued

base of the system (the last place which undergoing the melting process). Enlarging the surface area of the fins helps more convective heat to exchange with the PCM during the same time. On the one hand, because of generating the natural convection, circulation of the molten PCM is formed. On the other hand, the fins serve as a buffer against this movement, limiting the amount of free convection that occurs.

Figure 8 shows the temperature distribution contours in 2400 s for Cases 1–5. The temperature in the HTF channels remains constant (the temperature value is the same as the inlet temperature) due to the short

length of the system. The PCM temperature rises at the adjacent region to the wall and around the fins for all the cases. During the first 600 s, the fins could not reach the heat balance with the HTF since the fins gain heat from the HTF and deliver it to the PCM. Therefore, the fins' temperature is higher/lower than that of the PCM/HTF until all the PCM melts, then the system approaches thermal equilibrium. The center of each region between the neighbor fins in the PCM domain shows a colder temperature due to the relatively far distance from the wall. The PCM domain approaches the thermal equilibrium gradually, and due to the

natural convection and buoyancy effect, the top part of the region reaches thermal equilibrium. Within 2400 s, the average temperature for Case 5 reaches 49.8°C. Considering Cases 1 and 4, the average temperature reaches 43.3°C and 49°C, respectively. Because of the gathering of the solid PCM at the base of the unit, the temperature of that region records lower values than

that of the other regions. Overall, the average temperature is directly proportional to the number of fins, since the high number of fins provides a larger heat transfer surface area, which improves the conduction at the beginning of the melting mechanism and then improves the convection heat transfer due to the larger area for the heat transfer.

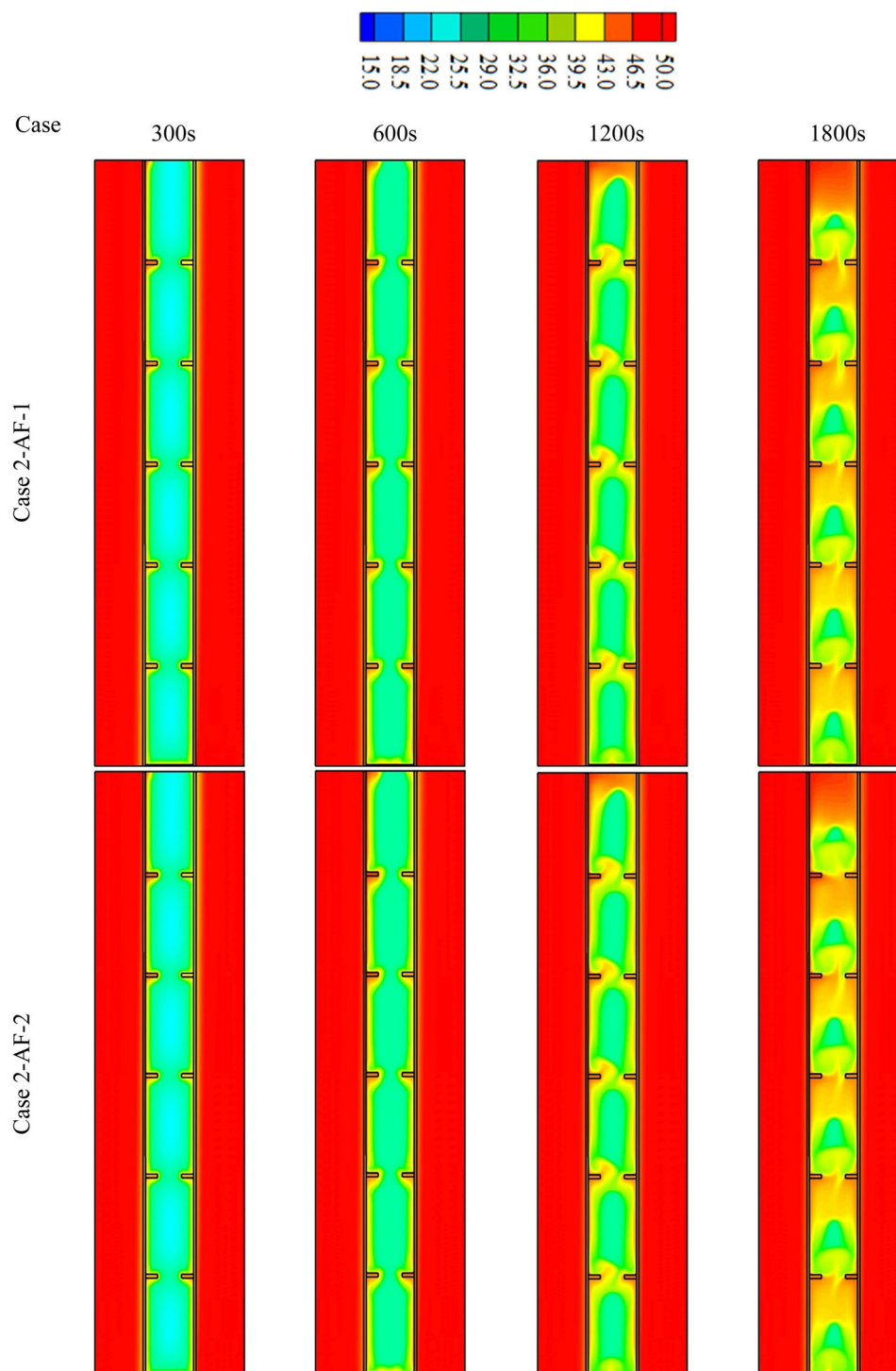


FIGURE 11 The temperature contours for Case 2-AF-1, Case 2-AF-2, Case 2-AF-3, and Case 2-AF-4.

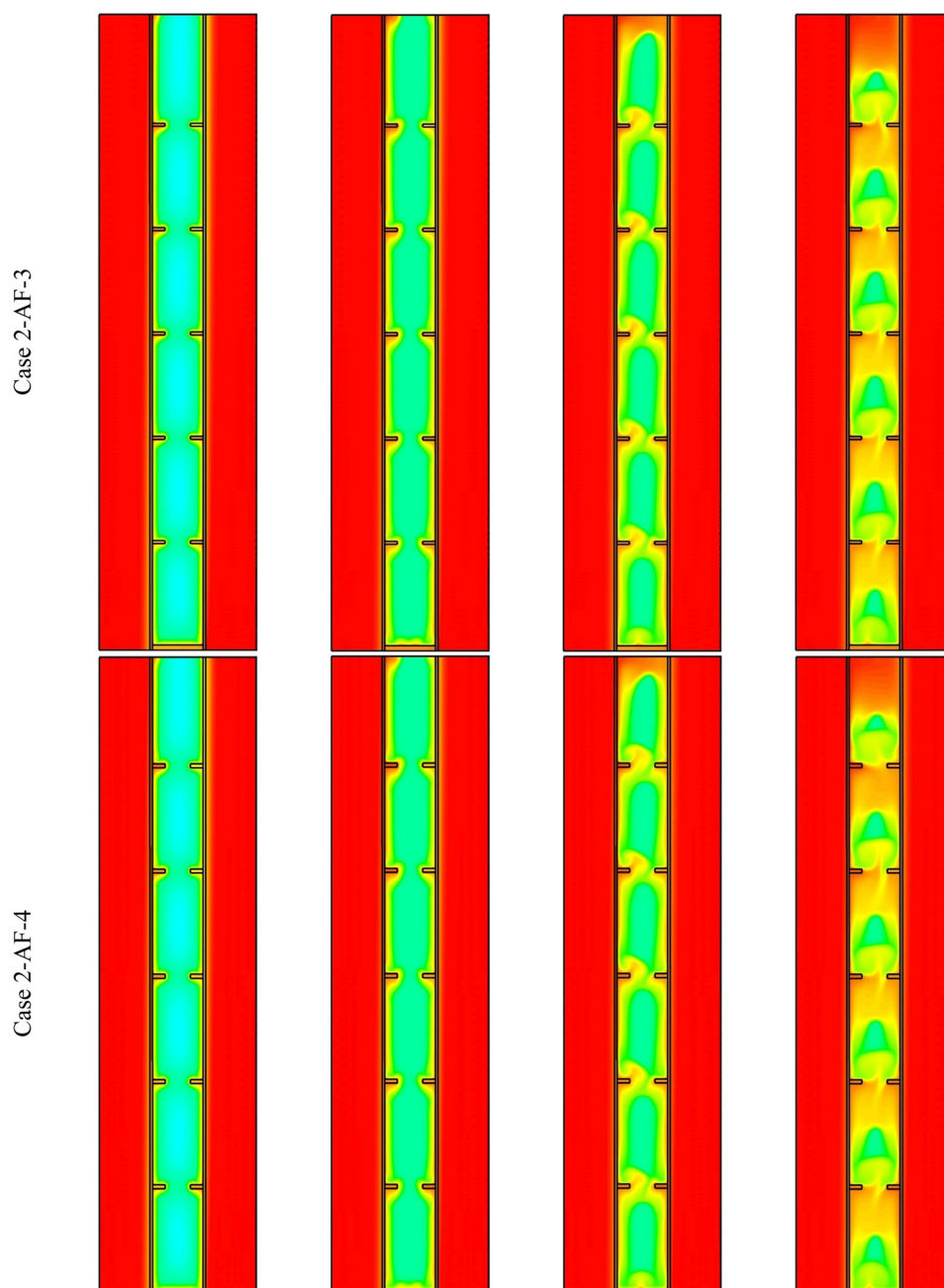


FIGURE 11 Continued

Figure 9A shows the development of the liquid fraction for Cases 1–5 during the entire melting process. The charging process occurs sharply within the first 600 s due to the conduction heat transfer with the solid PCM. The gradient of the melting process reduces slightly due to generating the natural convection heat transfer. When the liquid fraction achieves 93%, the curve shape changes to plateau for all the cases due to the domination of the natural convection at that stage. Case 1 shows the slowest phase-changing

TABLE 6 The total melting time and the heat storage rate for Case 2 with an added fin with different thicknesses.

	Melting time (s)	Heat storage rate (W)
Case 2-AF-1	2114	76.16
Case 2-AF-2	2079	77.24
Case 2-AF-3	2141	75.28
Case 2-AF-4	2078	77.24

process of all the cases. The fastest melting process occurs for Case 5 due to having the highest surface area. The average temperature sharply increases within the first 300 s because of the thermal conduction effect, as shown in Figure 9B. The natural convection is generated in the molten PCM near the region of the walls, and the fins cause a reduction in the warming rate of the PCM. The case with the highest number of fins (Case 5) has the highest average temperature value because of having the highest surface area and the PCM temperature reaches the thermal equilibrium within 2400 s. However, in Case 1, the thermal equilibrium reaches within 3500 s (46% slower compared with Case 5).

The melting time and heat storage rates are presented in Table 5 for Cases 1–5. Table 5 shows that the case with the highest number of fins (Case 5) is the best case among all the studied cases and the thermal performance of the system is proportional to the number of fins. This conduct can be attributed to two effects, first, increasing the number of fins increases the heat transfer surface area, which enhances the natural convection of the system. Second, the higher number of fins helps to distribute those fins more homogeneously in the system and the lower fin becomes closer to the base of the PCM domain, which accelerates the phase change process for the solid part that always remains at

the base. Case 1 is known as the worst case due to having the longest melting time and the lowest heat storage rate. The total melting time of the PCM in Case 5 is 2375 s, which is shorter than that of Cases 1, 2, 3, and 4 by 54.1%, 28.7%, 17.7%, and 10.6%, respectively. The heat storage rate of Case 5 (70.76 W) also shows an advantage compared with the other cases, which is higher than that of Cases 1, 2, 3, and 4 by 35%, 22.2%, 15%, and 9.5%, respectively. The outline of this section reveals that utilizing more fins offers a higher surface area of heat transfer resulting in a faster charging process and higher heat storage rate.

5.2 | Effect of the added fin to the bottom for the case with 5 fins

To evaluate the effects of the added fin thickness on the charging process, four different values (0.5, 1, 2, and the same thickness of the fins [mm]) are considered for the added fin thickness at the bottom of the system. This study is assessed by analyzing the contours of the liquid fraction and the temperature, the melting time, and the average heat storage of each case.

Figure 10 illustrates the liquid fraction development for the cases presented in Table 2 at various times of 300, 600, 1200, and 1800 s. For all the cases,

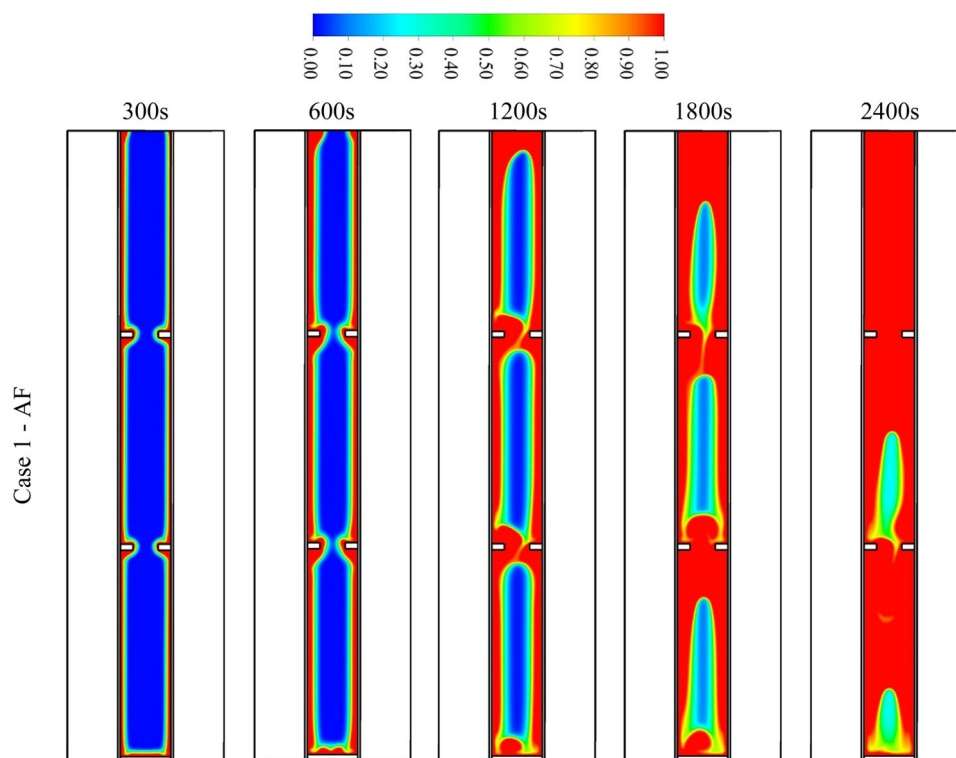


FIGURE 12 The liquid fraction development in Cases 1-AF, 2-AF, 3-AF, 4-AF, and 5-AF at different times.

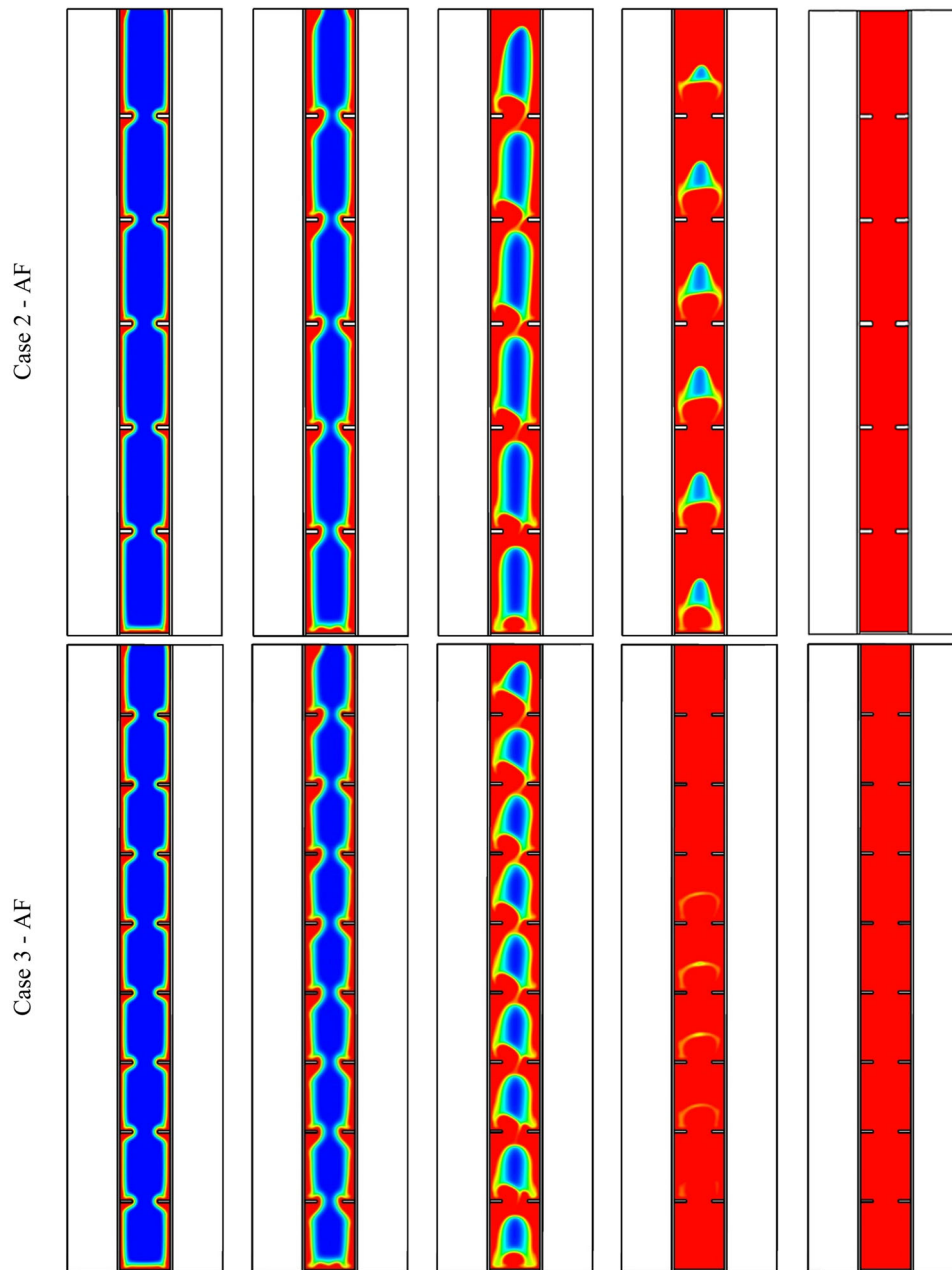


FIGURE 12 Continued

the PCM melting trends are almost similar. The phase change process launches beside the walls, around the fins, and above the added bottom fin (the area of collecting the solid state of the PCM). The thermal conduction controls phase change at the beginning of the charging process due to managing the heat transfer between the PCM and the solid metal. The molten PCM extends progressively over time due to gaining more heat from the walls and the fins. At the base part of the system, the phase change process of the PCM continuously occurs due to the adhesion

of the PCM to the flat fin. All the cases virtually show the same conduct, and the solid part is restricted between the two neighbor fins. Within the 1800 s, the actual differences between the cases could not be recognized, as all the cases behave similarly, and the differences appear after the mentioned time. For all the cases, around 90% of the PCM melts during the 1800 s. This behavior returns to the ignorable differences in the surface areas of the fins.

The temperature profile also can be affected by the added fin at the bottom of the system, as shown in

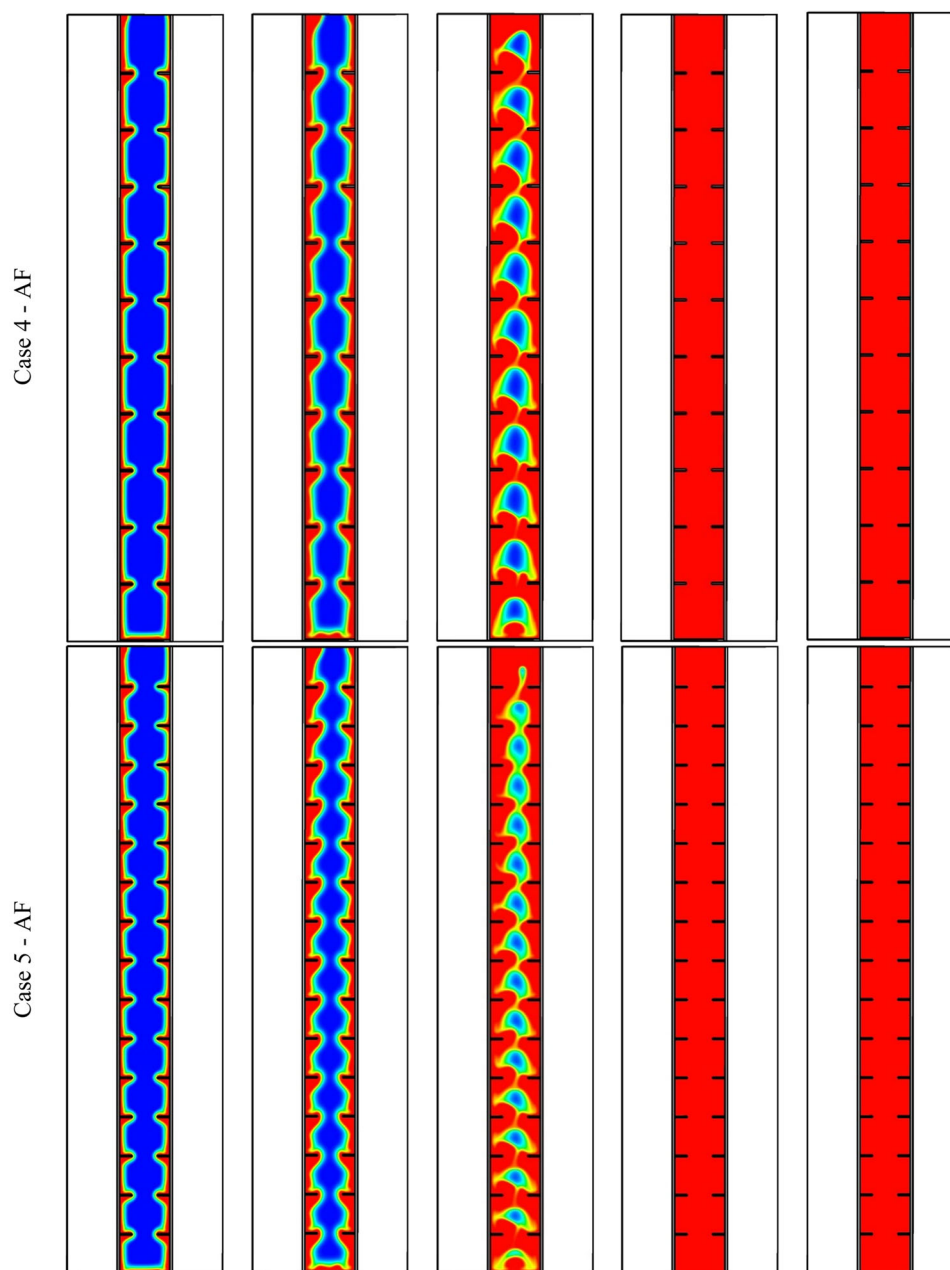


FIGURE 12 Continued

Figure 11. The figure indicates that the temperature values at the base of the heat exchanger rise due to the presence of the bottom fin. Thus, the mean temperature of the system increases compared to the cases without the added fin. Most of the warm PCM is collected at the top of the region between the fins, and overall, they are gathered at the top of the system which reaches the thermal equilibrium first.

Table 6 lists the results of the overall thermal storage rate and melting time for the cases covered in this section. The case with the unified thickness (Case 2-AF-

4) shows better performance compared with that of Case 2-AF-1, Case 2-AF-2, and Case 2-AF-3. However, compared with Case 2-AF-2 with the fin thickness of 1 mm, the difference is unnoticeable. The heat storage rate for the unified thickness case is equal to 77.24 W, which is higher than Case 2-AF-1 and Case 2-AF-3 by 1.4% and 2.5%, respectively. The melting time of the case with unified thickness is 2078 s, which is lower than Case 2-AF-2 by just 1 s, and shorter than the times recorded for Case 2-AF-1 and Case 2-AF-3 by 1.7% and 3%, respectively.

5.3 | Simultaneous effect of the added fin to the bottom and the number of fins

The unified thickness of the fins in the previous section showed the best performance among the other cases. Therefore, this case is considered for further case studies. The effect of the added fin at the bottom with the same thickness as the other fins on the melting process of the LHTES is analyzed in this section for the cases with various numbers of fins. The dimension of the fins is listed in Table 3. Since the volume of the fins in all cases are equal, the thickness of the fins reduces by increasing the number of fins, as shown in Table 1. For Case 1-AF, the thickness of the fins and the added fin is 2.5 mm. The melting process starts faster due to the process of the flat fin, because of its role in the melting of the solid phase at the base as shown in Figure 6. Within the time of, 2400 s, 95% of the total PCM is melted in Case 1-AF. Increasing the number of fins improves the melting process, since the surface area increases. Within 1800 s, 90% of the PCM is melted for Case 2-AF, and the PCM is totally melted in 78 s. For Cases 3-AF, 4-AF, and 5-AF, 99%, 100%, and 100% of the PCM are melted within 1800 s, respectively. Comparing these images with those in Figure 12 clearly shows that adding fins to the base of the PCM container enhances the phase change process properly due to enlarging the surface area on the one hand and

accelerating the melting process of the solid part at the bottom of the section on the other hand.

Figure 13 shows the temperature contours of Cases 1-AF, 2-AF, 3-AF, 4-AF, and 5-AF in the presence of a flat fin at the bottom. The temperature rises in the areas beside the wall and around the fins, whereas the top region of the PCM container reaches the heat balance first and this state expands downward. For Cases 1-AF and 2-AF, the temperature could not reach the thermal equilibrium within 2400 s, since some regions of the PCM are not melted during that period. However, for Case 3-AF, the average temperature reaches 45°C within 1800 s, causing 99% of the PCM to be melted. Increasing the number of the fins to 10 and 15 results in the melting of the entire PCM, and consequently, the unit reaches the thermal equilibrium within 1800 s.

Figure 14 shows the temperature- and the liquid fraction-time profile of the cases with an added flat fin to the base of the PCM container. Figure 14A illustrates that the temperature rises sharply for all the cases within the first 300 s due to the conduction effect. Convection heat transfer emerges in the system during the melting mode, slowing the rate of temperature rise. The heat exchange between the PCM and the solid walls reduces as a result of the development of liquid PCM with a relatively high temperature alongside the walls and around the fins, resulting in a decline in the temperature-increasing trend. Meanwhile, increasing the number of fins

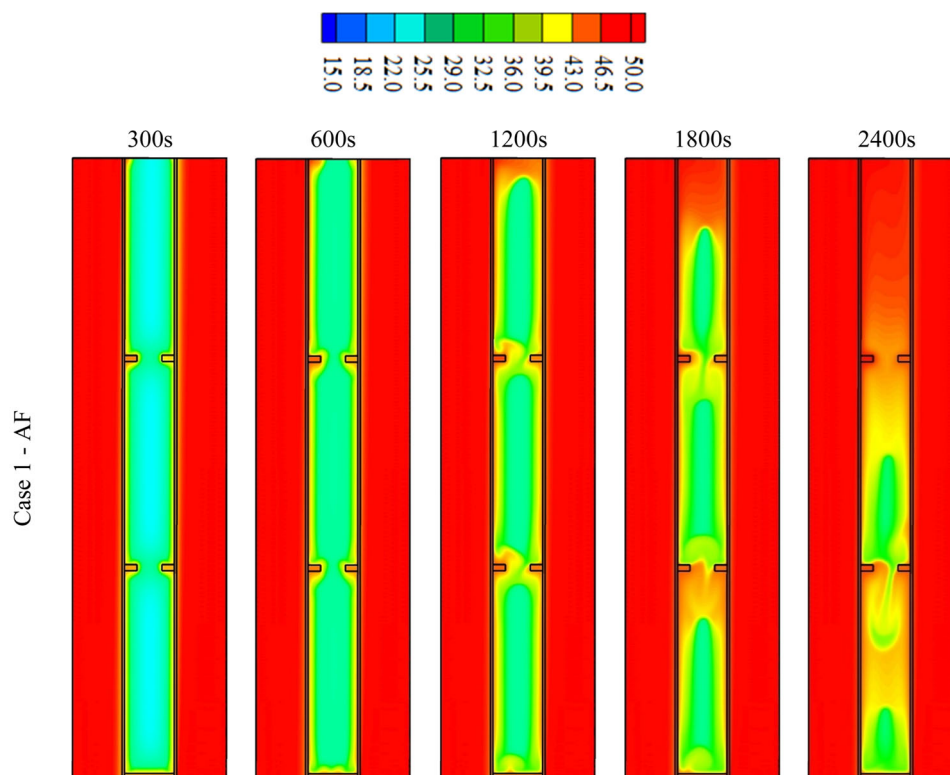


FIGURE 13 The temperature contour in Cases 1-AF, 2-AF, 3-AF, 4-AF, and 5-AF at different times.

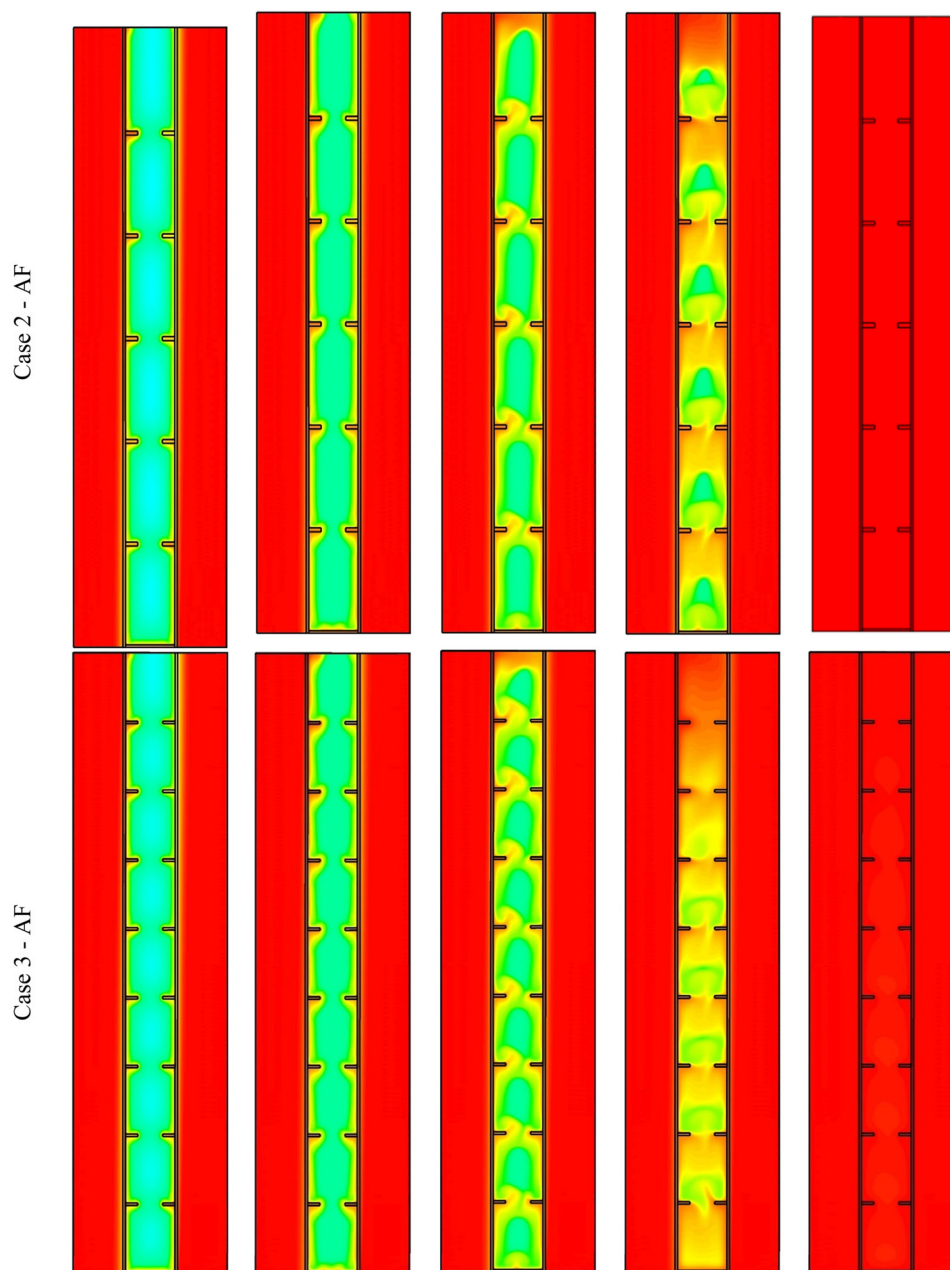


FIGURE 13 Continued

increases the surface area of the heat transfer, resulting in a higher rate of temperature rise. The PCM achieves thermal equilibrium in Cases 5-AF, 4-AF, and 1-AF in 2000, 2200, and 3400 s, respectively. Figure 14B depicts the growth of the liquid fraction during the melting process. Because of the fast heat transfer rate from the fins to the PCM, the melting process begins quickly and in a consistent manner in all situations, as seen in the figure. Because conduction is the primary heat transmission method, molten PCM develops differently in each situation. Increasing the number of fins causes the liquid fraction to grow more sharply.

Table 7 presents the melting time and the heat storage rate for Cases 1-AF to 5-AF. The total melting time for Case 5-AF is 1549 s, which is shorter than Cases 1-AF, 2-AF, 3-AF, and 4-AF by 85.8%, 34.2%, 18.1%, and 8.8%, respectively. The heat storage rate for Case 5-AF shows an advantage over the other cases (102.56 W), which is higher than the above-mentioned cases by 44%, 24.4%, 14.9, and 8.5%, respectively. The melting time for Case 5 without an added flat fin increases by 53.3% compared with that of Case 5-AF. Furthermore, the heat storage rate of Case 5 reduces by 31% compared with that of Case 5-AF. Overall, increasing the fin numbers and using a flat fin at the base of

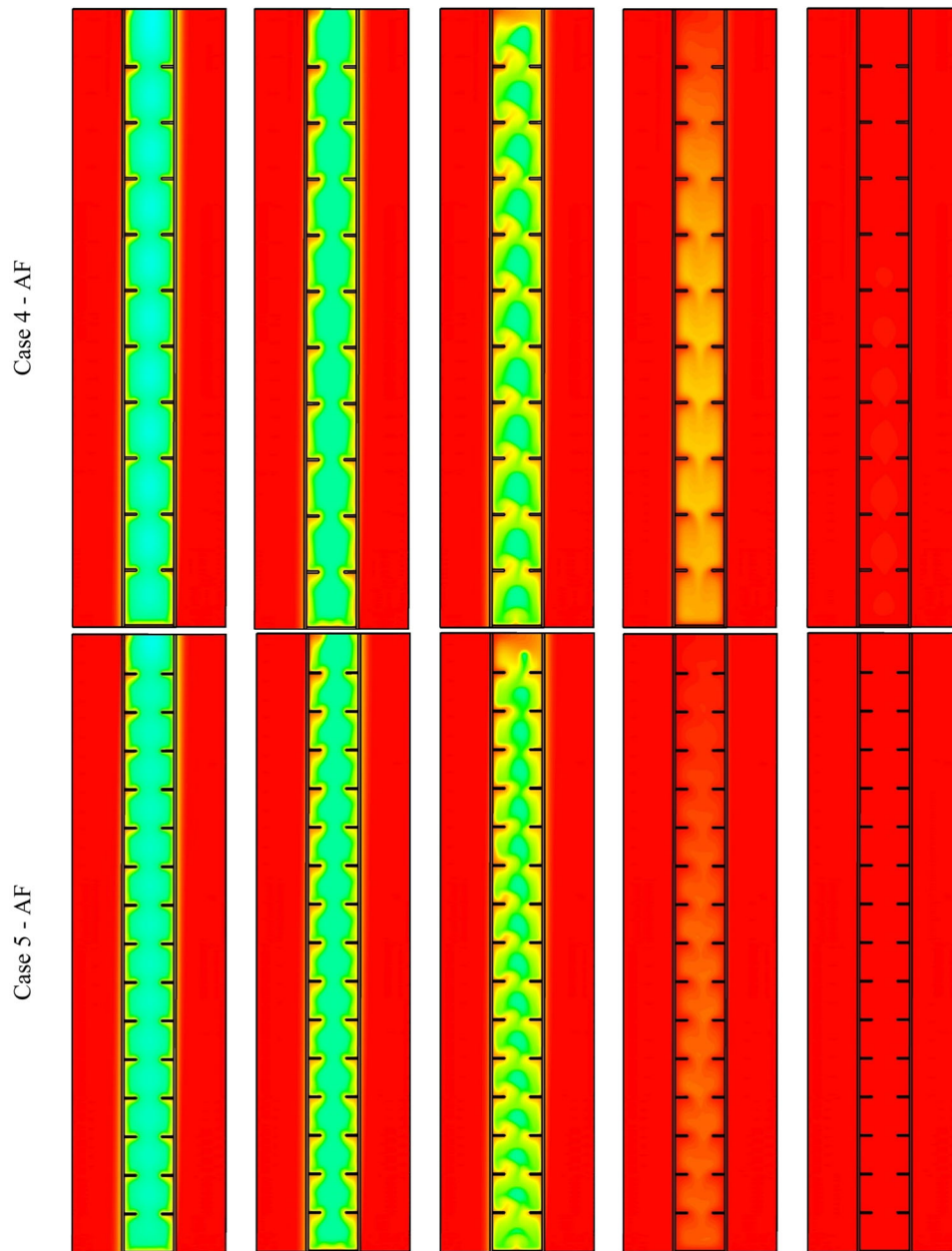


FIGURE 13 Continued

the system with a unified thickness have resulted in better thermal performance.

6 | CONCLUSION

The accelerated melting behavior of a PCM based on a triple-tube confinement design with internal annular fins was investigated in this study. The purpose was to explore how the number of fins and their locations with varying thicknesses and the addition of a bottom fin could impact the improved heat transport on the PCM side. Different fin configurations were evaluated

and compared in terms of melting completion, temperature distribution, melting time, and heat storage rate to determine the best fin number and thickness. Furthermore, the impact of adding a fin to the bottom of a heat exchanger of several thicknesses was explored. The main conclusions can be summarized as follows:

1. Applying more fins offers a higher surface area of heat transfer which results in a faster charging process and higher heat storage rate. The total melting time of the PCM in the case with 30 fins (without the added fin) is 2375 s, which is shorter than cases with 4, 10, 16, and

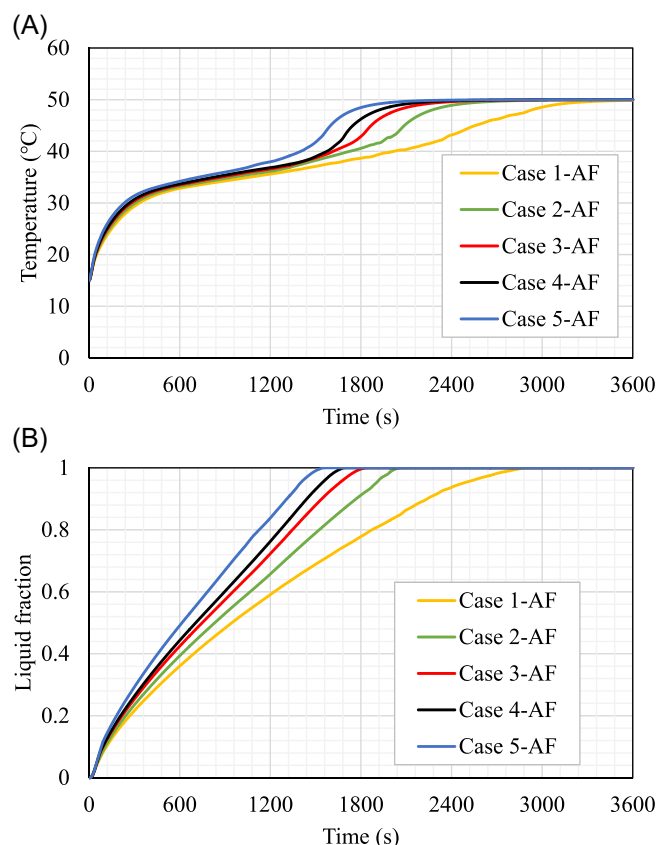


FIGURE 14 (A) Average temperature profiles and (B) liquid fraction profiles in Cases 1-AF, 2-AF, 3-AF, 4-AF, and 5-AF.

TABLE 7 The total melting time and the heat storage rate for the Cases 1-AF, 2-AF, 3-AF, 4-AF, and 5-AF.

	Melting time (s)	Heat storage rate (W)
Case 1-AF	2878	57.4
Case 2-AF	2078	77.56
Case 3-AF	1829	87.32
Case 4-AF	1686	93.88
Case 5-AF	1549	102.56

20 fins by 54.1%, 28.7%, 17.7%, and 10.5%, respectively. The heat storage rate for the case with 30 fins is 56.02 W, which is higher than the cases with 4, 10, 16, and 20 fins by 35%, 22.2%, 15%, and 9.5%, respectively.

- On the evaluation of adding a fin to the bottom of the heat exchanger, it was shown that the unified thickness of the fins (array fins and the added flat fin) shows better performance compared with the other added fin cases. The heat storage rate for the unified thickness case with 10 fins is 77.24 W, which is

higher than cases with the added fin thicknesses of 0.5 and 2 mm by 1.4% and 2.4%, respectively.

- The case with 30 fins equipped with a flat fin at the base of the PCM enclosure shows superior performance among all the studied cases. The total melting time for this case is 1549 s, which is shorter than the added fin cases with 4, 10, 16, and 20 fins by 85.8%, 34.2%, 18%, and 8.8%, respectively. The heat storage rate also shows an advantage for the case of 30 fins, which were found higher than the above-mentioned cases by 78.6%, 32.23%, 17.5%, and 9.2%, respectively.
- By eliminating the fin at the bottom of the system with 30 fins, the charging time increase by 53.3%, and the heat storage rate reduces by 45%, respectively.

ACKNOWLEDGMENT

The authors acknowledge help from Indrajit Patra and N. Bharath Kumar to carry out this study.

NOMENCLATURE

A_m	mushy zone
C_p	specific heat capacity, J/kg K
g	gravity, m/s ²
k	thermal conductivity, W/m K
L_f	latent heat, J/kg
M	mass, kg
P	pressure, Pa
Q	heat storage
t_m	melting/solidification time, s
T	temperature, K
S	term
\vec{V}	velocity, m/s

GREEK SYMBOLS

β	thermal expansion coefficient, K ⁻¹
λ	liquid fraction
μ	viscosity, kg/m s
ρ	PCM density, kg/m ³
ΔH	PCM latent heat, J/kg

ORCID

Jasim M. Mahdi  <http://orcid.org/0000-0002-6060-5015>

REFERENCES

- Zhang Y, Pan Z, Yang J, et al. Study on the suppression mechanism of (NH₄)₂CO₃ and SiC for polyethylene deflagration based on flame propagation and experimental analysis. *Powder Technol.* 2022;399:117193.
- Zhang X, Tang Y, Zhang F, Lee CS. A novel aluminum-graphite dual-ion battery. *Adv Energy Mater.* 2016;6(11):1502588.

3. Lu C, Liu Q, Zhang B, Yin L. A Pareto-based hybrid iterated greedy algorithm for energy-efficient scheduling of distributed hybrid flowshop. *Expert Syst Appl*. 2022;204:117555.
4. Pan Q, Zheng Y, Tong Z, Shi L, Tang Y. Novel lamellar tetrapotassium pyromellitic organic for robust high-capacity potassium storage. *Angew Chem Int Ed*. 2021;60(21):11835-11840.
5. Sefidan AM, Taghilou M, Mohammadpour M, Sojoudi A. Effects of different parameters on the discharging of double-layer PCM through the porous channel. *Appl Therm Eng*. 2017;123:592-602.
6. Veerakumar C, Sreekumar A. Phase change material based cold thermal energy storage: materials, techniques and applications—a review. *Int J Refrig*. 2016;67:271-289.
7. Kamkari B, Shokouhmand H, Bruno F. Experimental investigation of the effect of inclination angle on convection-driven melting of phase change material in a rectangular enclosure. *Int J Heat Mass Transfer*. 2014;72:186-200.
8. Mohammed HI. Discharge improvement of a phase change material-air-based thermal energy storage unit for space heating applications using metal foams in the air sides. *Heat Transfer*. 2022;51(5):3830-3852.
9. Mahdi JM, Lohrasbi S, Nsofor EC. Hybrid heat transfer enhancement for latent-heat thermal energy storage systems: a review. *Int J Heat Mass Transfer*. 2019;137:630-649.
10. Yin H, Han C, Liu Q, Wu F, Zhang F, Tang Y. Recent advances and perspectives on the polymer electrolytes for sodium/potassium-ion batteries. *Small*. 2021;17(31):2006627.
11. Li Z, Peng M, Zhou X, et al. In situ chemical lithiation transforms diamond-like carbon into an ultrastrong ion conductor for dendrite-free lithium-metal anodes. *Adv Mater*. 2021;33(37):2100793.
12. Yang X, Wang X, Liu Z, Luo X, Yan J. Effect of fin number on the melting phase change in a horizontal finned shell-and-tube thermal energy storage unit. *Sol Energy Mater Sol Cells*. 2022;236:111527.
13. Guo J, Wang X, Yang B, Yang X, Li MJ. Thermal assessment on solid-liquid energy storage tube packed with non-uniform angled fins. *Sol Energy Mater Sol Cells*. 2022;236:111526.
14. Guo J, Liu Z, Yang B, Yang X, Yan J. Melting assessment on the angled fin design for a novel latent heat thermal energy storage tube. *Renew Energy*. 2022;183:406-422.
15. Tang S, Zhou J, Shen C, Zhang D. Thermal performance analysis and optimization of melting process in a buried tube latent heat storage system. *J Energy Storage*. 2022;52:104863.
16. Shahsavari A, Goodarzi A, Mohammed HI, Shirneshan A, Talebizadehsardari P. Thermal performance evaluation of non-uniform fin array in a finned double-pipe latent heat storage system. *Energy*. 2020;193:116800.
17. Ismail K, Alves C, Modesto M. Numerical and experimental study on the solidification of PCM around a vertical axially finned isothermal cylinder. *Appl Therm Eng*. 2001;21(1):53-77.
18. Agyenim F, Eames P, Smyth M. A comparison of heat transfer enhancement in a medium temperature thermal energy storage heat exchanger using fins. *Sol Energy*. 2009;83(9):1509-1520.
19. Mosaffa AH, Talati F, Basirat Tabrizi H, Rosen MA. Analytical modeling of PCM solidification in a shell and tube finned thermal storage for air conditioning systems. *Energy Build*. 2012;49:356-361.
20. Al-Abidi AA, Mat S, Sopian K, Sulaiman MY, Mohammad AT. Internal and external fin heat transfer enhancement technique for latent heat thermal energy storage in triplex tube heat exchangers. *Appl Therm Eng*. 2013;53(1):147-156.
21. Mahdi JM, Nsofor EC. Solidification enhancement of PCM in a triplex-tube thermal energy storage system with nanoparticles and fins. *Appl Energy*. 2018;211:975-986.
22. Guo J, Du Z, Liu G, Yang X, Li MJ. Compression effect of metal foam on melting phase change in a shell-and-tube unit. *Appl Therm Eng*. 2022;206:118124.
23. Sardari PT, Mohammed HI, Giddings D, Walker GS, Gillott M, Grant D. Numerical study of a multiple-segment metal foam-PCM latent heat storage unit: effect of porosity, pore density and location of heat source. *Energy*. 2019;189:116108.
24. Liu X, Mohammed HI, Ashkezari AZ, Shahsavari A, Hussein AK, Rostami S. An experimental investigation on the rheological behavior of nanofluids made by suspending multi-walled carbon nanotubes in liquid paraffin. *J Mol Liq*. 2020;300:112269.
25. Mahdi JM, Nsofor EC. Melting enhancement in triplex-tube latent heat energy storage system using nanoparticles-metal foam combination. *Appl Energy*. 2017;191:22-34.
26. Zhang L, Huang M, Xue J, Li M, Li J. Repetitive mining stress and pore pressure effects on permeability and pore pressure sensitivity of bituminous coal. *Nat Resour Res*. 2021;30(6):4457-4476.
27. Chamkha A, Doostanidezfuli A, Izadpanahi E, Ghalambaz M. Phase-change heat transfer of single/hybrid nanoparticles-enhanced phase-change materials over a heated horizontal cylinder confined in a square cavity. *Adv Powder Technol*. 2017;28(2):385-397.
28. Ghalambaz M, Doostani A, Chamkha AJ, Ismael MA. Melting of nanoparticles-enhanced phase-change materials in an enclosure: effect of hybrid nanoparticles. *Int J Mech Sci*. 2017;134:85-97.
29. El Hasadi Y, Khodadadi J. Numerical simulation of solidification of nanoparticle-enhanced phase change materials (NEPCM) considering transport of suspensions. Paper presented at: Proceedings of the International Symposium on Thermal and Materials Nanoscience and Nanotechnology. 2011.
30. Xin C, Li Z, Zhang Q, Peng Y, Guo H, Xie S. Investigating the output performance of triboelectric nanogenerators with single/double-sided interlayer. *Nano Energy*. 2022;100:107448.
31. Ghalambaz M, Mehryan SAM, Hajjar A, Veismoradi A. Unsteady natural convection flow of a suspension comprising nano-encapsulated phase change materials (NEPCMs) in a porous medium. *Adv Powder Technol*. 2020;31(3):954-966.
32. Ho CJ, Liu YC, Ghalambaz M, Yan WM. Forced convection heat transfer of nano-encapsulated phase change material (NEPCM) suspension in a mini-channel heatsink. *Int J Heat Mass Transfer*. 2020;155:119858.
33. Wu N, Zhou X, Kidkhunthod P, Yao W, Song T, Tang Y. K-ion battery cathode design utilizing trigonal prismatic ligand field.

34. Zhang D, Zhang F, Tang S, Guo C, Qin X. Performance evaluation of cascaded storage system with multiple phase change materials. *Appl Therm Eng.* 2021;185:116384.
35. Fang M, Chen G. Effects of different multiple PCMs on the performance of a latent thermal energy storage system. *Appl Therm Eng.* 2007;27(5):994-1000.
36. Hu Z, Li A, Gao R, Yin H. Enhanced heat transfer for PCM melting in the frustum-shaped unit with multiple PCMs. *J Therm Anal Calorim.* 2015;120(2):1407-1416.
37. Mahdi JM, Mohammed HI, Hashim ET, Talebizadehsardari P, Nsofor EC. Solidification enhancement with multiple PCMs, cascaded metal foam and nanoparticles in the shell-and-tube energy storage system. *Appl Energy.* 2020;257:113993.
38. Bazai H, Moghimi MA, Mohammed HI, Babaei-Mahani R, Talebizadehsardari P. Numerical study of circular-elliptical double-pipe thermal energy storage systems. *J Energy Storage.* 2020;30:101440.
39. Sharifi N, Faghri A, Bergman TL, Andracka CE. Simulation of heat pipe-assisted latent heat thermal energy storage with simultaneous charging and discharging. *Int J Heat Mass Transfer.* 2015;80:170-179.
40. Mehryan SAM, Vaezi M, Sheremet M, Ghalambaz M. Melting heat transfer of power-law non-Newtonian phase change nano-enhanced n-octadecane-mesoporous silica (MPSiO₂). *Int J Heat Mass Transfer.* 2020;151:119385.
41. Ghalambaz M, Hashem Zadeh SM, Mehryan SAM, Pop I, Wen D. Analysis of melting behavior of PCMs in a cavity subject to a non-uniform magnetic field using a moving grid technique. *Appl Math Model.* 2020;77:1936-1953.
42. Lohrasbi S, Sheikholeslami M, Ganji DD. Multi-objective RSM optimization of fin assisted latent heat thermal energy storage system based on solidification process of phase change material in presence of copper nanoparticles. *Appl Therm Eng.* 2017;118:430-447.
43. Gasia J, Maldonado JM, Galati F, De Simone M, Cabeza LF. Experimental evaluation of the use of fins and metal wool as heat transfer enhancement techniques in a latent heat thermal energy storage system. *Energy Convers Manag.* 2019;184: 530-538.
44. Wang W, He X, Shuai Y, Qiu J, Hou Y, Pan Q. Experimental study on thermal performance of a novel medium-high temperature packed-bed latent heat storage system containing binary nitrate. *Appl Energy.* 2022;309:118433.
45. Mao Q, Zhang Y. Thermal energy storage performance of a three-PCM cascade tank in a high-temperature packed bed system. *Renew Energy.* 2020;152:110-119.
46. Yang J, Liu H, Ma K, Yang B, Guerrero JM. An optimization strategy of price and conversion factor considering the coupling of electricity and gas based on three-Stage game. *IEEE Trans Autom Sci Eng.* 2022;1-14.
47. Hosseini MJ, Ranjbar AA, Rahimi M, Bahrampoury R. Experimental and numerical evaluation of longitudinally finned latent heat thermal storage systems. *Energy Build.* 2015;99:263-272.
48. Wang P, Yao H, Lan Z, Peng Z, Huang Y, Ding Y. Numerical investigation of PCM melting process in sleeve tube with internal fins. *Energy Convers Manag.* 2016;110:428-435.
49. Yazici MY, Avci M, Aydin O. Combined effects of inclination angle and fin number on thermal performance of a PCM-based heat sink. *Appl Therm Eng.* 2019;159:113956.
50. Kalbasi R, Afrand M, Alsarraf J, Tran MD. Studies on optimum fins number in PCM-based heat sinks. *Energy.* 2019;171:1088-1099.
51. Yan W-T, Ye W-B, Li C. Effect of aspect ratio on saturated boiling flow in microchannels with nonuniform heat flux. *Heat Transfer.* 2019;48(7):3312-3327.
52. Yan W-T, Li C, Ye W-B. Numerical investigation of hydrodynamic and heat transfer performances of nanofluids in a fractal microchannel heat sink. *Heat Transfer.* 2019;48(6): 2329-2349.
53. Yao S, Huang X. Study on solidification performance of PCM by longitudinal triangular fins in a triplex-tube thermal energy storage system. *Energy.* 2021;227:120527.
54. Sodhi GS, Muthukumar P. Compound charging and discharging enhancement in multi-PCM system using non-uniform fin distribution. *Renew Energy.* 2021;171:299-314.
55. Wang G, Feng L, Altanji M, Sharma K, Sooppy Nisar K, Khorasani S. Proposing novel "L" shaped fin to boost the melting performance of a vertical PCM enclosure. *Case Stud Therm Eng.* 2021;28:101465.
56. Desai AN, Shah H, Singh VK. Novel inverted fin configurations for enhancing the thermal performance of PCM based thermal control unit: a numerical study. *Appl Therm Eng.* 2021;195:117155.
57. Mao Q, Li Y, Li G, Badiei A. Study on the influence of tank structure and fin configuration on heat transfer performance of phase change thermal storage system. *Energy.* 2021;235:121382.
58. Mao Q, Hu X, Li T. Study on heat storage performance of a novel vertical shell and multi-finned tube tank. *Renew Energy.* 2022;193:76-88.
59. Sardari PT, Walker GS, Gillott M, Grant D, Giddings D. Numerical modelling of phase change material melting process embedded in porous media: effect of heat storage size. *Proc Inst Mech Eng A J Power Energy.* 2019;234(3): 365-383.
60. Mat S, Al-Abidi AA, Sopian K, Sulaiman MY, Mohammad AT. Enhance heat transfer for PCM melting in triplex tube with internal-external fins. *Energy Convers Manag.* 2013;74: 223-236.
61. Ye W-B, Zhu D-S, Wang N. Numerical simulation on phase-change thermal storage/release in a plate-fin unit. *Appl Therm Eng.* 2011;31(17):3871-3884.
62. Assis E, Katsman L, Ziskind G, Letan R. Numerical and experimental study of melting in a spherical shell. *Int J Heat Mass Transfer.* 2007;50(9):1790-1804.
63. Sardari PT, Giddings D, Grant D, Gillott M, Walker GS. Discharge of a composite metal foam/phase change material to air heat exchanger for a domestic thermal storage unit. *Renew Energy.* 2020;148:987-1001.
64. Waldrop JM, Song B, Patkowski K, Wang X. Thermal energy charging behaviour of a heat exchange device with a zigzag plate configuration containing multi-phase-change-materials (m-PCMs). *Appl Energy.* 2015;142:328-336.
65. Li ZX, Al-Rashed AAAA, Rostamzadeh M, Kalbasi R, Shahsavari A, Afrand M. Heat transfer reduction in

buildings by embedding phase change material in multi-layer walls: effects of repositioning, thermophysical properties and thickness of PCM. *Energy Convers Manag.* 2019;195:43-56.

66. Xu Y, Ren Q, Zheng ZJ, He YL. Evaluation and optimization of melting performance for a latent heat thermal energy storage unit partially filled with porous media. *Appl Energy.* 2017;193:84-95.

How to cite this article: Bahlekeh A, Mohammed HI, Al-Azzawi WK, et al. CFD analysis on optimizing the annular fin parameters toward an improved storage response in a triple-tube containment system. *Energy Sci Eng.* 2022; 1-26. doi:10.1002/ese3.1310